Fall 12-10-2019

Interpreting amalgamation processes of a fluvial sandstone of the Nacimiento Formation in the San Juan Basin, New Mexico

Keely Elizabeth Miltenberger
University of New Mexico - Main Campus

Keely E. Miltenberger
Candidate

Earth and Planetary Sciences
Department

This thesis is approved, and it is acceptable in quality and form for publication:

Approved by the Thesis Committee:

Dr. Gary Weissmann, Chairperson

Dr. Peter Fawcett

Dr. Louis Scuderi

INTERPRETING AMALGAMATION PROCESSES OF A FLUVIAL SANDSTONE OF THE NACIMIENTO FORMATION IN THE SAN JUAN BASIN, NM

by

KEELY MILTENBERGER

BACHELOR OF SCIENCE IN EARTH AND PLANETARY SCIENCES

THESIS

Submitted in Partial Fulfillment of the
Requirements for the Degree of

Master of Science in
Earth and Planetary Sciences

The University of New Mexico
Albuquerque, New Mexico

May, 2020

ACKNOWLEDGEMENTS

I would like to sincerely thank the many people that helped me with my research. My family has been very patient and supported me through the last two years, thank you to my husband Luke, and sons Addison and Quentin. A huge thank you to my advisor, Dr. Weissmann and the remainder of my graduate committee, Dr. Fawcett, and Dr. Scuderi. Many thanks to Wade, Karen, Quentin, and Dustin who helped me immensely with field work. I would also like to thank the administration, we would be lost without Faith, Paula, Mabel, and Cecilia! Thank you to Jed Frescette for taking the time to meet with me and for introducing me to Houdini. Thank you to my fellow graduate students and best friends, Jessica, Christina, and Johanna for moral and friendly support!! Thank you to all of my fellow coworkers and friends at the United States Geological Survey for supporting me through my degree(s)! Lastly, I would like to thank the New Mexico Geological Society for a generous graduate student grant to help offset research costs.

Interpreting amalgamation processes of a fluvial sandstone of the Nacimiento Formation in the San Juan Basin, NM

Keely Miltenberger

Bachelor of Science in Earth and Planetary Sciences

Master of Science in Earth and Planetary Sciences

ABSTRACT

Outcrop studies of fluvial sand bodies are important for the study of fluid transport and storage capabilities because the deposits are heterogeneous. 3-D photogrammetry was used to evaluate the amalgamation processes of a multi-storey sheet sandstone in the San Juan Basin, NM. The Angel Peak member was deposited in the proximal-medial transition of a distributive fluvial system by a meandering river during the Paleocene. Within the study area, amalgamation occurred by avulsion and reoccupation of channel-belts to produce five storeys of the multi-storey sheet sandstone. Within each storey is evidence of processes that are internal to a channel-belt, such as bar migrations, small scour surfaces, and chute deposits. Vertical truncation by subsequent channel-belts has occurred to each storey. Miocene to present erosion has also removed portions of the uppermost storeys within the detailed study area. The multi-storey sheet sandstone of the Angel Peak member was deposited as the San Juan Basin was almost full, thus has many characteristics of amalgamation during low accommodation space.

LIST OF FIGURES

LIST OF TABLES

TABLE OF CONTENTS

INTRODUCTION

Internal structure of fluvial sandstone bodies offers clues to how the sandstone developed due to river channel migration, provides insights to paleogeography, and provides the heterogeneous structure through which subsurface fluids migrate, causing dispersion of contaminants in aquifer systems and compartmentalization of petroleum reservoirs. Outcrop studies provide insights into the internal structure and heterogeneity of such sandstone bodies, and modern 3-D photogrammetric analysis can help build a greater understanding of geometric relationships in these sandstone bodies. The purpose of this study is to evaluate the amalgamation processes that produced a multi-storey sheet sandstone (MSSS) of the Nacimiento Formation in the San Juan basin (SJB). More specifically, to (1) assess the efficacy of applying 3-D photogrammetry to conducting alluvial architecture studies, (2) determine how this multi-storey sandstone developed and (3) to measure internal structure geometries of a multi-storey sheet sandstone in the medial-proximal transition zone of a distributive fluvial system (DFS) to provide geometric measurements for aquifer and reservoir models.

Gibing (2006) defined a multi-storey sandstone as an arrangement of superimposed vertical and lateral sandstone channel bodies. Sheet sandstones form through migration and accretion of sediments in laterally mobile rivers (Miall, 1996). Sheet sandstones can form as complex fill deposits or by simple sheetflood deposits and may reflect intervals of low stream power, steady discharge, or weak riverbanks (Friend, 1979; Miall, 1996). Most mobile channel-belt sheet sandstones have a width/thickness (W/T) of at least 15 and typically well above 100 (Miall, 1996; Gibling, 2006).

Amalgamation processes

A review of fluvial sandstone literature regarding avulsion and amalgamation processes of multi-storey sandstones offers three primary endmembers for amalgamation– amalgamation via internal processes, amalgamation by avulsion and reoccupation, and amalgamation due to confinement of the channel-belt (Bridge, 2003; Chamberlin and Hajek, 2015; Chamberlin, 2016).

Internal processes

Amalgamation can occur within a single channel-belt to produce an MSSS and is considered to occur because of internal processes acting within the fluvial system (Figure 1a). Seasonal fluctuations in discharge can cause sinuosity changes, lateral migration, accretion, and erosion to occur within a single channel-belt (e.g., Slingerland and Smith, 2004; Chamberlin and Hajek, 2015; Owen, et al., 2015; Durkin et al., 2017). Internal processes within a channel-belt can encompass many processes, such as migration of unit bars, cutbank erosion, local channel avulsions, scour surfaces, meander cut-offs, and (or) neck and chute cut-offs within the channel-belt. Fluvial bars are considered the main depositional component element of fluvial systems (a.k.a. channel-belts) and they represent downstream and vertical accretion (Allen, 1983; Chakraborty, 1999). Bars are depositional features that sit higher than the streambed and may become exposed subaerially during low flow conditions (Allen, 1993; Chakraborty, 1999). The deposits of a meandering channel-belt become more complex with time because internal processes have an opportunity to act over a longer period and overprint older deposits (Durkin et al., 2018). The study of modern meander-belts shows that over time, repeated intra-channel-belt processes cause overprinting of deposits especially closer to the belt axis (Durkin et al., 2017). This creates a direct relationship between the occupation time of a channel-belt and the complexity of the deposits (Durkin et al., 2018).

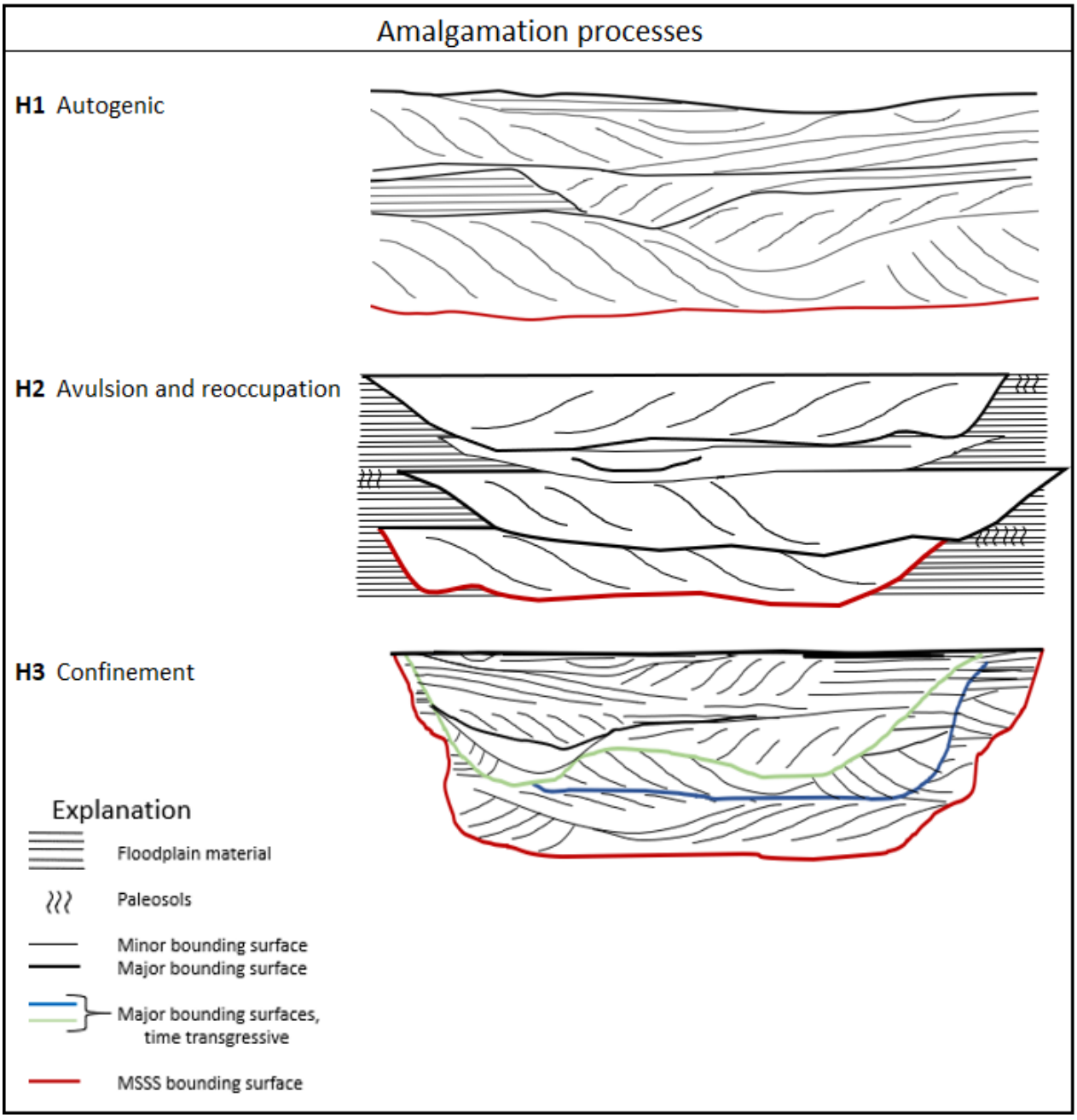

Figure 1. Three end-member possibilities for amalgamation of MSSS. H1) internal, H2) avulsion and reoccupation, and H3) confinement. Time transgressive bounding surfaces indicated in green and blue, MSSS bounding surface indicated in red.

If the MSSS was amalgamated by multiple channels within a single channel-belt, the following features are expected to be observed within the sheet sandstone (Figure 1a): short scour lengths (compared to bar lengths), bar or channel migrations (gently dipping lateral accretion sets), smooth sheet sandstone bounding surface, and evidence for meander cut-offs, and cuts and fills

(Chamberlin, 2016). Chamberlin (2016) also noted that there may be alluvial ridges and crevasse splay deposits within the sandstone. A relatively thin MSSS width, thin storeys, and a small number of storeys would be expected for internal processes because all amalgamation occurred within one channel-belt. According to Gibling (2006), a very narrow or narrow sheet sandstone is less than 100 meters in width.

Avulsion and reoccupation

The second process in which to amalgamate a MSSS involves regional or nodal avulsions and reoccupation of former channel belt positions. The MSSS formed by this process consists of amalgamated stacked channel-belts (Figure 1b). A common mechanism in which fluvial systems alter their course is by avulsions. Avulsions are geomorphic processes in which a river diverts some or all of its flow to the adjacent floodplain when there is even minimal aggradation occurring (Slingerland and Smith, 2004). They tend to occur on cutbanks of meander bends (Slingerland and Smith, 2004) and can shift upstream as the alluvial ridges become higher over time (Mackey, et al., 1995).

Slingerland and Smith (2004) proposed three different ways in which flow is diverted and an avulsion occurs. The first occurs by annexation (reoccupation), in which flow is diverted to an active or inactive channel with a higher gradient (Slingerland and Smith, 2004). The second is by incision, where new channels erode into the adjacent floodplain and the third is by progradation, where discharge expands laterally, reduces its carrying capacity, and forms a sediment wedge that migrates downstream (Slingerland and Smith, 2004).

Chamberlin and Hajek (2015) found that stratigraphically, avulsions of the channel-belt occur in three main styles, random, compensational, or clustered, though these are not directly linked to

the three avulsion types of Slingerland and Smith (2004). Channel-belt relocation by the random style occurs with equal probability that the channel-belts would avulse anywhere on the DFS (Chamberlin and Hajek, 2015). The compensational style occurs by relocation of channel-belts toward the lowest elevation on the DFS, typically avoiding locations of previous channel-belt occupation (Hofman et al., 2011; Chamberlin and Hajek, 2015). Clustered avulsion style occurs when channel-belts avulse to previously occupied locations (Chamberlin and Hajek, 2015). Hofman et al (2011) found that clustered and compensationally stacked channel-belts in the Piceance Basin in Colorado formed over different time intervals. Clustered channel-belts form over tens to 100s of thousand years, while compensational stacking occurs over a much longer time period of about 400 thousand years, and channel-belts usually stack more evenly (Hofman et al., 2011; Benhallam et al., 2016).

Features for amalgamation through avulsion and reoccupation may include long scour lengths (compared to bar lengths), flood plain material and paleosols associated with each storey, clay-clast conglomerates near storey bases, sawtooth storey edges, an irregular sheet sandstone bounding surface, a small number of storeys, or a variable number of storeys within the sheet sandstone (e.g., Holbrook, 2000; Chamberlin and Hajek, 2015; Chamberlin, 2016) (Figure 1b).

Confinement

The third processes by which to make a MSSS is by confinement of a channel-belt within an incised valley (Figure 1c) (e.g., Weissmann et al., 2002, 2015; Gibling, et al., 2005; Gibling, 2006; Chamberlin, 2016). Amalgamation by this process would occur when a river incises a valley but later becomes aggradational and is confined within the container valley (Gibling, 2006). This style of amalgamation has been strongly linked to cycles of incision and aggradation (Weissmann et al., 2002; Gibling et al., 2005; Gibling, 2006; Fontana et al., 2008).

Features for this form of amalgamation may include down-cutting through container overbank deposits below and adjacent to the sheet sandstone, lag deposits near storey contacts, steep-sided sheet sandstone edges, low W/Ts, and floodplain or paleosol deposits associated with entire sheet sandstone (Chamberlin, 2016) (Figure 1c).

For this study, I tested if field and 3-D alluvial architecture studies could be used to determine which process(es): internal (H1), avulsion and reoccupation (H2), or confinement (H3) likely acted to amalgamate the MSSS in the Nacimiento Formation at the study site. For the amalgamation of the MSSS to have occurred in the proximal to medial transition of a DFS, I hypothesized that amalgamation was predominantly by avulsion and reoccupation (H2).

BACKGROUND

Basin sedimentation

Tectonics, climate change, glaciation, and internal processes are mechanisms that affect fluvial systems within a DFS (Weissmann, et al., 2002; Fontana et al., 2008; Gibling et al., 2005; Gibling et al., 2011). When a fluvial system responds to a tectonic or climatic perturbation it experiences a complex response, in that it adjusts its profile by aggrading or eroding to achieve a system equilibrium (Bull, 1991).

Uplift, subsidence, and differential subsidence can occur extra- and intra- basin from orogenic events, faulting, or glacial eustasy (Gibling, 2006). Sediment supply and discharge are strongly affected by climate and therefore impact the cycles of aggradation and incision within sedimentary basins (Bull, 1991; Weissmann, et al., 2002; Fontana et al., 2008; Gibling, 2011). Tectonics and changes to climate cause variation in the ratio of available accommodation space

to sediment supply (A/S) in the basin, which in turn determines if deposition or erosion will occur (Leeder, 2009).

High A/S intervals have been found to have both higher channel-belt slopes and higher sinuosities; successions tend to exhibit vertical aggradation and low channel-belt clustering (Benhallam et al., 2016). This produces an alluvial architecture of predominantly narrow sheet sandstones and steer-head channels encased in floodplain material (Kjemperud et al., 2008). The character of these deposits is very similar to the distal deposits found in a DFS because distal areas have more accommodation space available to fill.

Conversely, low accommodation space intervals have been found to have lower channel-belt slopes (Mackey, et al., 1995), basinward DFS lengthening (Weissmann et al., 2013), higher net-to-gross sand ratios (Mackey, et al., 1995), and thus a greater degree of amalgamation. The resultant architecture is predominantly wide sheet sandstones formed by increased channel-belt clustering (Benhallam et al., 2016), and may exhibit scouring, and cannibalization (Kjemperud et al., 2008).

Distributive fluvial systems (DFS)

Weissmann et al. (2010, 2011, 2015) showed that continental fluvial basin fill is dominated by DFSs, comprised of alluvial fans, fluvial megafans, alluvial plains, or bajadas. A common vertical succession of facies has been identified within DFS deposits, which occurs by progradation of a DFS over time (Weissmann et al., 2013; Owen et al 2015a, b). Progradation of the DFS and concurrent filling of the basin results in an upward vertical coarsening of facies and higher degrees of amalgamation (Figure 2) (Weissmann et al., 2013; Owen et al 2015a, b). Relative to proximal deposits, medial DFS deposits may have greater preservation of fine-

grained sediments, levee and avulsion deposits, and more widely spaced channel-belts; they are considered to be the 'transition zone' between proximal and distal facies (Weissmann, et al., 2013). Distal facies are fine grained, groundwater fed, and poorly drained, and as a result, wetland areas are common to distal portions of a DFS (Weissmann et al., 2013; 2015). Progradation of a DFS over time results in distal, fine-grained, and poorly drained paleosol facies being overlain by medial and proximal facies that are coarser and better drained (Figure 2) (Weissmann et al., 2013).

Amalgamated channel-belts are most common in the proximal areas of a DFS and the medial to proximal transition can be identified in a vertical succession by the lowest amalgamated sandstone (Figure 2).

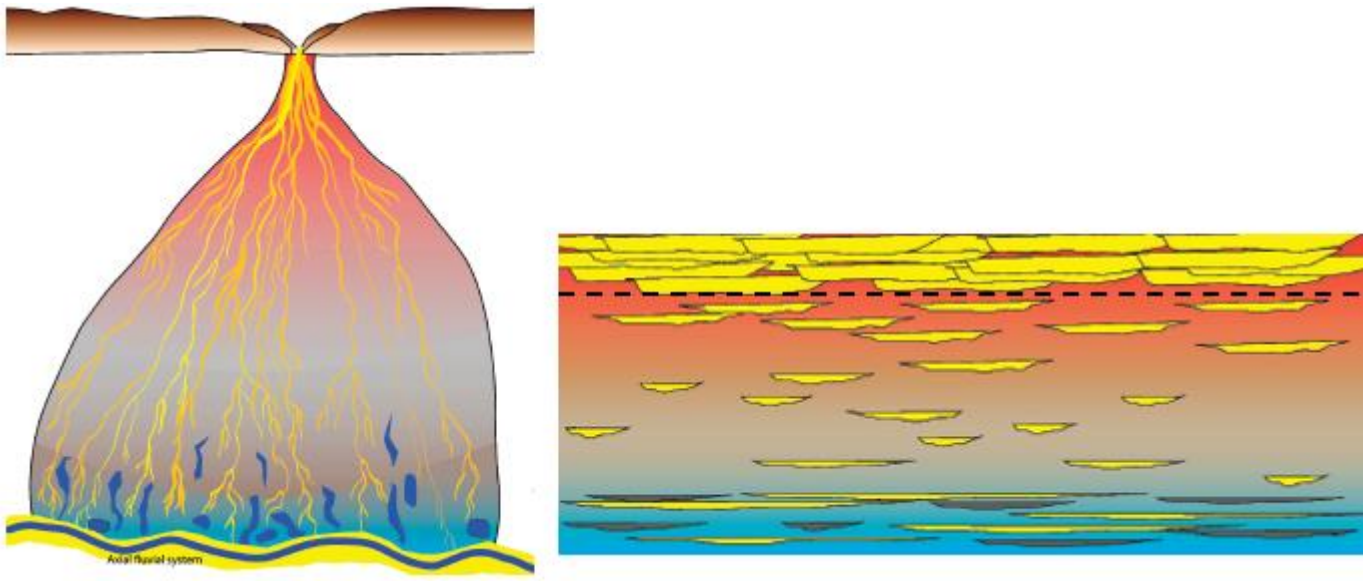

Figure 2. Modified schematic planview and hypothetical cross section of a DFS (Weissmann et al., 2013). Dashed line indicates transition between proximal and distal facies (Weissmann et al., 2013).

Study Area

San Juan Basin

The San Juan Basin (SJB) is an asymmetrical broken foreland basin located on the eastern margin of the Colorado Plateau in northwestern New Mexico (Figure 3) (Baltz, 1967; Cather, 2004). The Laramide Orogeny in northern New Mexico began during the retreat of the Cretaceous Interior Seaway, around 78-75 Ma and continued until approximately 35 Ma (Cather, 2004; Cather et al., 2012). Flat slab subduction of the Farallon plate under what is now the western Unites States caused volcanism and cycles of uplift that formed the San Juan and La Plata uplifts in southern Colorado (Sikkink, 1987). Subsidence of the SJB occurred in three separate phases throughout the Laramide Orogeny – (1) the late Cretaceous, (2) the late Cretaceous-early Paleocene, and (3) the Eocene (Cather, 2004). During the late Cretaceous and much of the Paleogene, fluvial clastic rocks from the San Juan and La Plata uplifts were transported by south flowing rivers and deposited in the SJB (Baltz, 1967; Williamson, 1993; Cather, 2004; Cather et al., 2019). Fluvial Paleocene rocks include the McDermott, Animas, Ojo Alamo, and Nacimiento Formations (McDermott and Animas are equivalent formations to Ojo Alamo and Nacimiento in Colorado) (Figure 3) (Williamson, 1993; Cather, 2004). Clastic sediments included exhumed crystalline igneous and metamorphic rocks and eroded Paleozoic sedimentary rocks that formerly capped the San Juan Mountains (Sikkink, 1987).

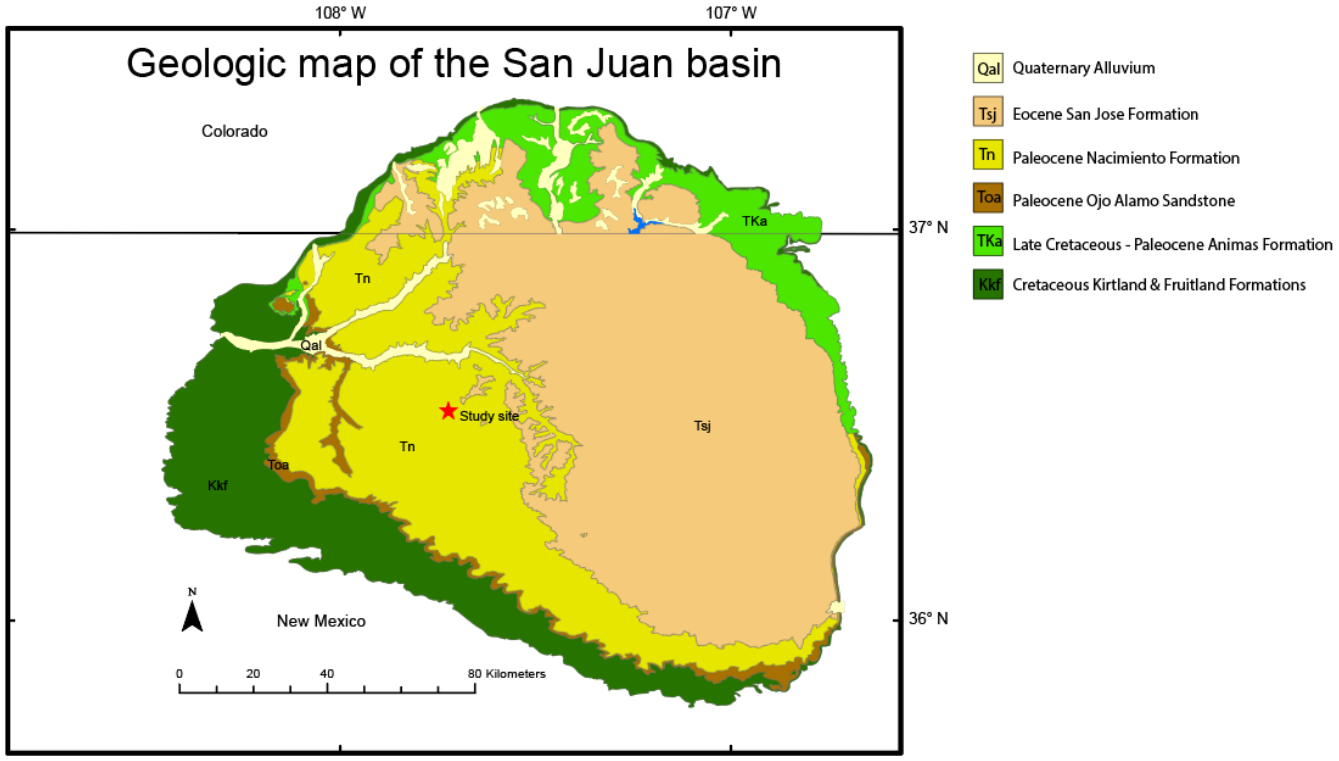

Figure 3. Location and geology of the San Juan basin in New Mexico & Colorado (modified from Green, 1992 and Geologic map of NM, 2003).

The SJB has experienced approximately one kilometer of exhumation by erosion that began approximately 15 Ma (Braschayko, 2008; Cather, 2012). Erosion resulted in numerous drainages cut through SJB fluvial deposits, leaving mesas of resistant sandstones, gently sloping hills of overbank deposits, and badland topography.

Nacimiento Formation

Surficial and subsurface deposits of the Nacimiento Formation (Tn) can be found throughout much of the SJB (Figure 3). Study of the Paleocene Nacimiento Formation is of great interest because fluvial deposition occurred near the K-Pg extinction event and contains two unique mammalian faunas that are the type location for the study of their diversification (Williamson and Lucas, 1996). As a result, many studies have been conducted to constrain more precise geochronological ages for the formation. Results of recent studies provide the age estimate of

65.7-63 Ma for the Nacimiento Formation (Williamson and Lucas, 1993; Cather, 2004; Leslie et al., 2018). Through study of the paleosols and paleoflora of the Paleocene fluvial deposits within the SJB, Hobbs (2016) suggested that the climate was consistently humid throughout deposition. There is a trend observed of better-drained paleosols and coarser deposits moving up section and thus DFS progradation is the currently accepted model for SJB deposition (Hobbs, 2016; Donahue, 2016; Leslie et al., 2018; Cather et al. 2019).

The majority of the Nacimiento Formation is composed of fluvial fine-grained deposits; however, it also contains sand bodies and MSSSs (Williamson, 1993). In northern portions of the basin, near the interpreted sediment source areas, the Nacimiento Formation can contain more than 50 percent sandstone (Baltz, 1967). In the central portion of the SJB, early Nacimiento rocks consist of thick successions of variegated fine-grained deposits but further up in section a noticeable transition to more sand bodies and the MSSS is observed. These findings are consistent with the DFS progradation model (Weissmann et al., 2013) and agree with Hobbs' (2016) findings for progradation of the basin. The Nacimiento Formation is up to 500 meters thick (Cather, 2004) and is thought to have been deposited as the accommodation space in the SJB was being reduced (Hobbs, 2016; Leslie et al., 2018; Cather et al. 2019).

Williamson (1993) assigned members to the Tn based on lithofacies, and include the Arroyo Chijuillita, Ojo Encino, Kutz, Unnamed, and Escaveda members (Figure 4). Cather et al. (2019) recently renamed the Unnamed member, the Angel Peak member (Tnap). Taylor (1977) identified three black layers in the Nacimiento formation within the Kutz Canyon area as black carbonaceous clays and suggested that their presence indicates a paludal environment for deposition (Taylor, 1977).

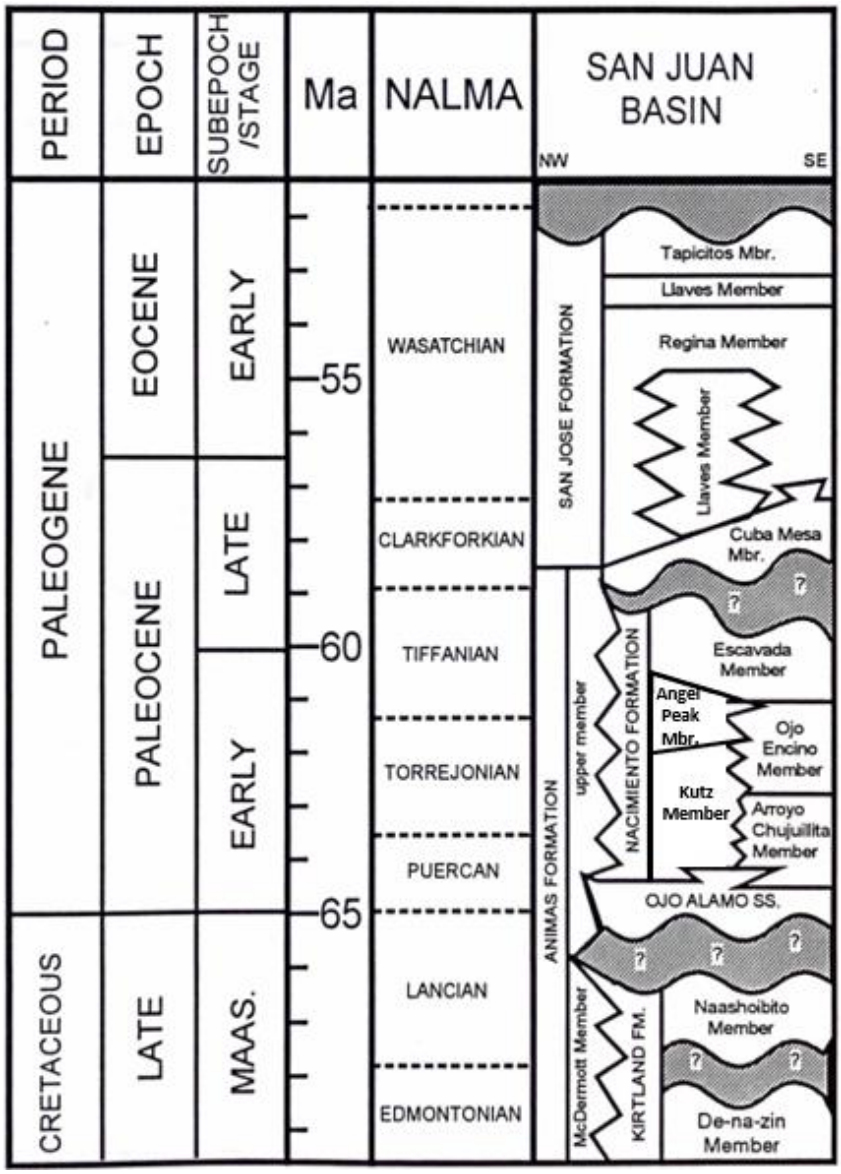

Figure 4. Stratigraphic column and nomenclature for SJB (modified from Williamson, 1993).

Carritt (2014) used terrestrial lidar to measure the dip at a site approximately 6.7 km southwest of the study area in Kutz Canyon to be only 0.295 degree toward the northwest. Carritt (2014) estimated an accumulation rate of 0.19 mm per year and a recurrence interval for fluvial avulsions of the Nacimiento to be every 34 thousand years. He made these calculations based on the thickness of the Nacimiento in Kutz Canyon and an interval of 0.75 million years for deposition (Carritt, 2014).

Angel Peak member of Nacimiento Formation (Tnap)

The Angel Peak member of the Nacimiento Formation is described in the west central SJB (Figures 4 and 5), between the lower Kutz and upper Escavada members (Williamson, 1993; Cather et al., 2019). The Angel Peak member was formerly identified as the 'unnamed member' and was only recently renamed the Angel Peak member (Cather et al., 2019). It is a multi-storey, cliff-forming sheet sandstone that is up to 70 meters thick (Williamson, 1993; Cather et al., 2019). The Angel Peak member interfingers with the Kutz member and thins distally to red beds in west-central NM (Williamson, 1993; Cather et al., 2019). The MSSS of the Angel Peak member is believed to have been deposited in the medial to proximal area of a prograding DFS (Hobbs, 2016).

Petrographic studies of Tn sandstones have been described as fine-to-medium grained, moderate-to-well sorted, angular-to-rounded feldspathic arenites (Hobbs, 2016). The only published paleo current data for the Angel Peak member comes from a very recent study, in which they found a dominant flow direction toward the east (n = 100) (Cather et al., 2019).

To study the development and internal structure of the Angel Peak MSSS, we selected an excellent 3-D exposure located in the central portion of the basin, just north of Angel Peak, and just east of Kutz Canyon (Figure 5). The MSSS is present in a double canyon outcrop that provides many views of the MSSS and internal structures. The detailed study site was the primary focus area used to interpret amalgamation processes that developed the MSSS of the Tnap. However, observing the storey edges was important for determining geometries and it was discovered early on that the detailed study area would need to be expanded to locate edges. Storey edges were located on the east and west side of the detailed study area (purple ovals in Figure 5).

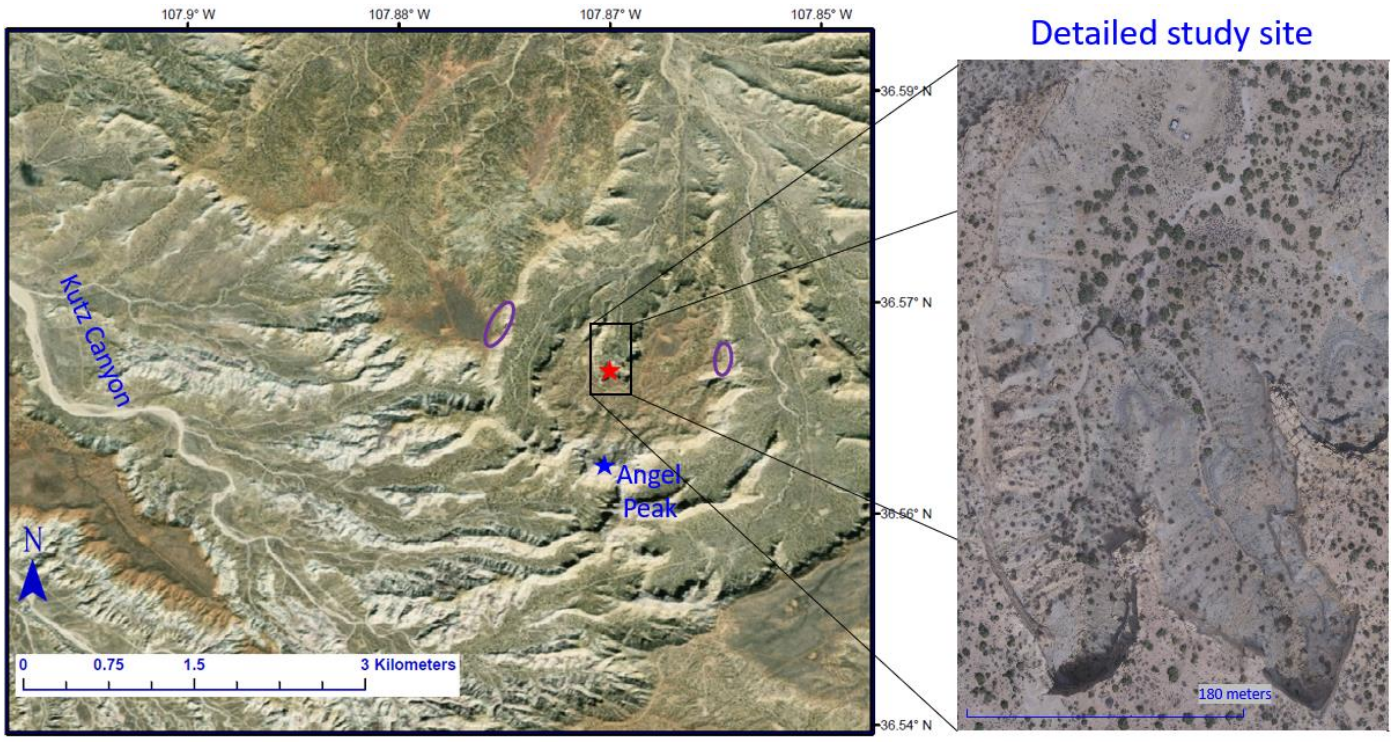

Figure 5. Detailed study area, expressed in relation to Angel Peak and Kutz Canyon, near the central part of the SJB. Purple ovals indicate locations where storey edges were located, just to the east and west of the detailed study area.

METHODS

The advent of unmanned aircraft systems (UAS), structure-from-motion, and image processing software enabled the analysis and correlation of bounding surfaces around the complex outcrop in the study area MSSS. This aided in distinguishing the fluvial amalgamation process for the Angel Peak member in the SJB. UASs allow access to areas that otherwise would not be accessible and provide additional angles for visualization that would otherwise not be captured by traditional means. Combined with traditional ground-based photography, quantitative measurements can be made on inaccessible areas of cliff faces. Photogrammetry and 3-D architecture analysis techniques of digital outcrops provide a new method to identify and correlate bounding surfaces and assign a hierarchy to the bounding surfaces, especially around corners or on complex outcrop areas.

Data Acquisition

Images of the study area were collected on multiple visits. Images were captured using a Phantom 4 drone, a near-infrared multispectral camera, and digital single-lens reflex (DSLR) cameras (Table A1). Images were collected in raw (uncompressed) and compressed (jpg) format and were geotagged with the capture location. Vertical cliffs were photographed near dawn or dusk or under cloudy conditions to avoid shadow effects.

Along with images, observations of the sandstone cliff faces were made during several field visits. Sandstone grain size, sorting, and sedimentary structures were documented. Binoculars were used to identify fine sedimentary structures where inaccessible. Paleocurrent indicators in the form of crossbedding were measured in the field with a Brunton Pocket Transit Compass. Orientations of lateral accretion sets and petrified log concretions were measured and used to compare to crossbedding directions. Perpendicular to dip lateral accretion and bearing line directions were chosen based on the dominant crossbedding direction for that storey. If paleocurrent indicators were not assessible, I positioned myself as close to parallel to the strike of the feature as possible.

Several images were selected for panoramas and used for initial drafting of bounding surfaces in the field. Panoramic images were created using Image Composite Editor v2.0.3.0 software and drafting was later performed in Adobe Illustrator v23.0.1.

Data Processing

Images that were collected with the Nikon camera were converted from NEF to TIFF formats before any image processing was performed. Image processing and 3-D outcrop model construction was accomplished through structure-from-motion processing in Agisoft Photoscan

v1.4.5 software with the parameters contained in Table A2. Two separate models were made in Photoscan – (1) a planview compilation from UAS images of approximately 0.64-km^2 and (2) ground-based/UAS model using imagery from the SLR and the UAS to include detail of the vertical cliffs in the study area. All geotoagged images were aligned and optimized in Photoscan. Dense point clouds, meshes, textures, and a digital elevation model were constructed in PhotoScan. Finished models were exported in wavefront file (obj) formats, with textures. To avoid large rounding errors when importing the latter, shifts were applied to model coordinates (Table A2) (pers. comm. Jed Freschette, 2018).

Several different software programs used for 3-D visualization and correlation were downloaded and trialed. These programs included Blender v2.79b, Lime v1.1, and Houdini FX v17.5.173. Houdini was ultimately selected because it was able to perform all required tasks for the project completion.

The model of the vertical cliffs and the texture were imported into Houdini for alluvial architecture analysis (Miall, 1996). Major bounding surfaces were drafted onto cliff face surfaces at the storey contacts. The bounding surfaces were 'PolyExtruded' across the study area (planes were projected in Houdini). Planes were projected perpendicular to the cliff faces and used to correlate around corners and across valleys in the 3-D outcrop model. Constant elevation was maintained by constraining the z-values of the bounding surfaces and their corresponding projected planes because a negligible dip was measured by Carritt (2014).

Major bounding surfaces/storeys were identified by locating and correlating flood plain deposits and clay-clast lag deposits for all exposures. Where storey edges could be observed, they were classified as sawtooth, steep-sided, or erosional (Figure 6). For reasons explained later, additional edges were sought out, from outside of the detailed study area, but are within 660

meters of the detailed study area (Figure 5). Major bounding surfaces were identified and assigned different colors and numbers to help visualize and make interpretations (Figure A1). All geometric measurements of the MSSS were performed in 3-D space using Photoscan and Houdini.

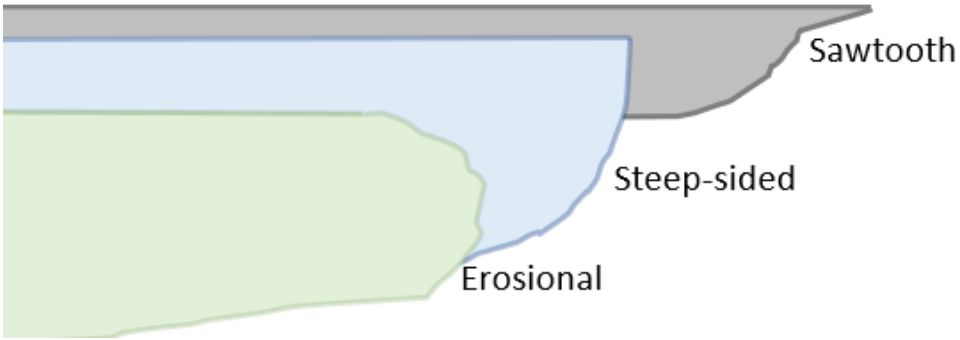

Figure 6. Storey edge classifications used for this study.

X, Y, Z point locations were obtained approximately every 5 meters along major bounding surfaces throughout the outcrop model in Houdini. Point locations were converted to raster format and subtracted from each other using the raster calculator tool in ArcMap v10.5.1. This provided discrete thicknesses and thickness ranges for each storey. Mean elevation values for each bounding surface were used to calculate the magnitude in which that elevation differs from the bounding surface mean elevation. The differences from the mean were used as elevation values to interpolate 3-D surfaces for each major bounding surface (Figure 8). Interpolation was performed using the Kriging tool in ArcMap because it is the best method for interpolating clustered discrete data. Once each bounding surface was interpolated, they were exported as 3-D object vrml files in ArcScene (Figure 7), converted to ply files using MeshLab (Paolo et al., 1999), and imported back into Houdini. This provided 3-D basal bounding surfaces that could be compared, measured, and used to quality check interpretations.

Figure 7. Kriged surfaces for the base of each storey in ArcScene. Each layer separated by 10 meters vertically for better storey visualization.

3-D Storey distribution analysis

Channel-belt deposits were identified and correlated in Houdini by projecting major bounding surfaces as planes. At least five storeys are present within the MSSS (Figure 8).

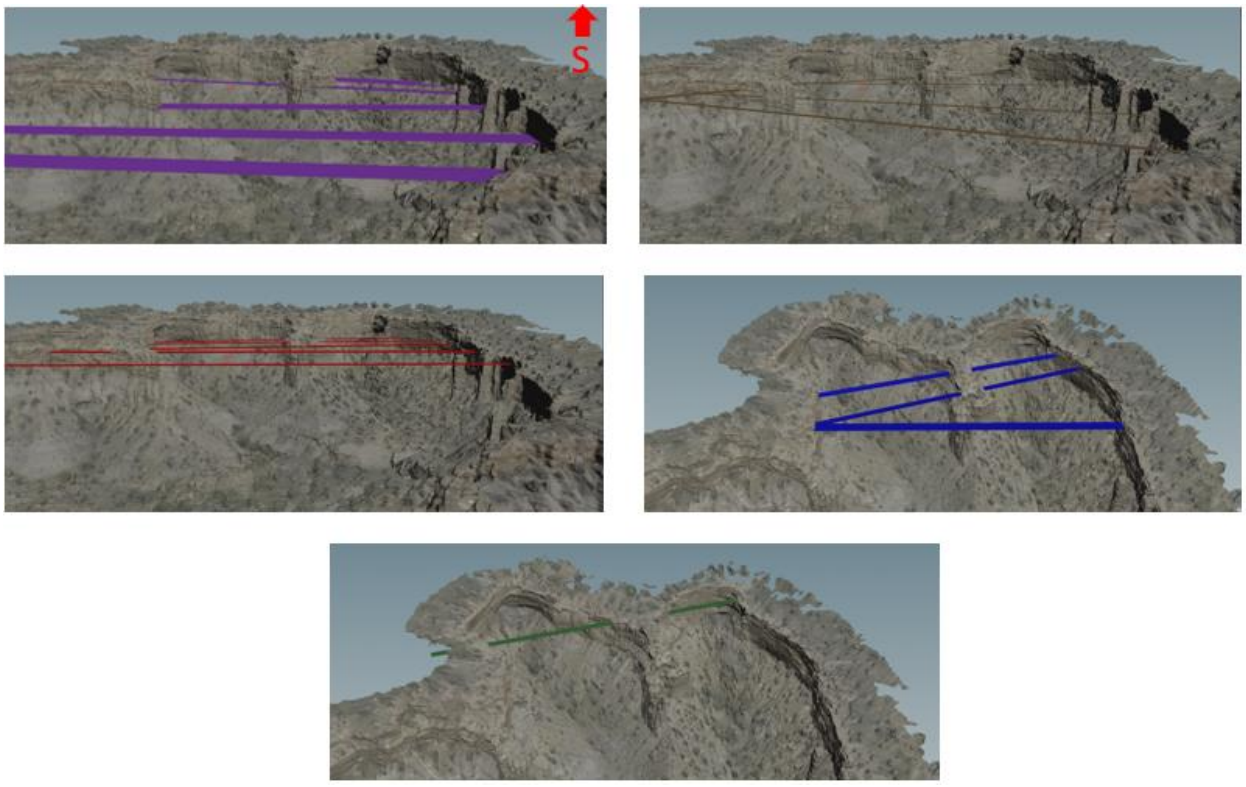

Figure 8. Initial major bounding surface projections and correlations in 3-D.

RESULTS AND INTERPRETATIONS

The MSSS is predominantly composed of channel-belt sandstones but contains other facies that represent different lithologies and depositional environments. Although paleosols are abundant throughout the SJB, none were observed in the MSSS.

Facies

Channel-belt sandstone

The sandstone is a weakly cemented feldspathic arenite-to-wacke. It is well sorted, moderate- to coarse-grained with thin gravel and pebble lenses further up the section (Figure 9c). Plane bedding and planar and trough crossbedding occurs within the channel-belt sandstone facies. Planar and trough crossbedding (Figure 9a & b) is present throughout the MSSS and was measured for paleocurrent directions in each storey.

Figure 9. Sedimentary structures of channel-belt sandstone, a) planar crossbedding, b) trough crossbedding, c) gravel to pebble lenses.

Lateral accretion sets

Large low angle lateral accretion sets with mud drapes occur within the MSSS (Figure 10) and indicate deposition by a meandering river. Lateral accretion sets can be an indicator of paleo-river stage because the inclined strata extend from the highest point on the cutbank, to the lowest point in the channel (Allen, 1968; Nichols, 2013). Two lateral accretion sets are interpreted to have been of the main channel have thicknesses of 8.62 and 12.2 meters, thus indicating that the MSSS was likely deposited by a laterally migrating river with a minimum channel depth of 8.62 to 12.2 meters (Allen, 1983; Chakraborty, 1999; Bridge, 2003).

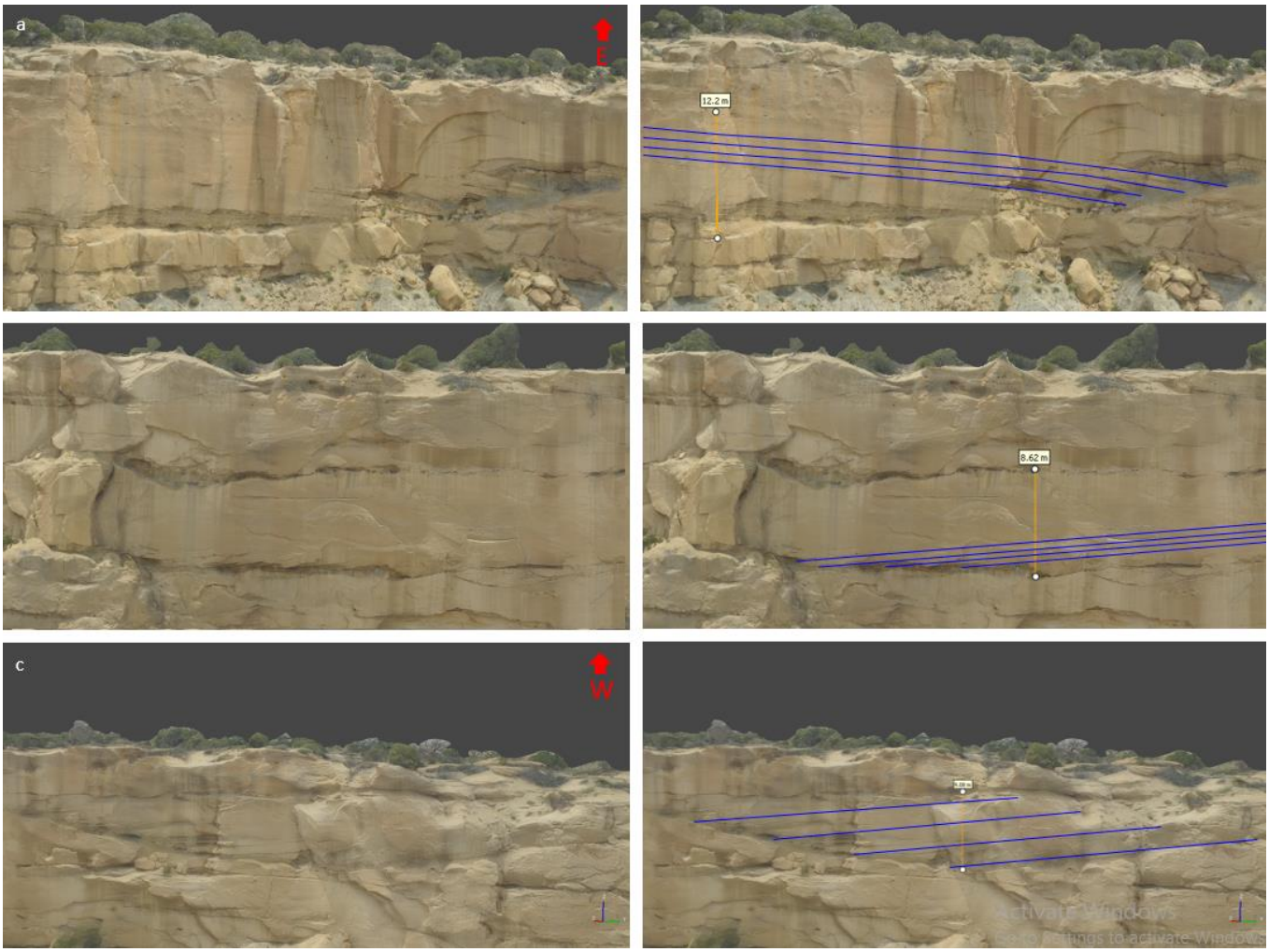

Figure 10. Undrafted and drafted images of outcropping lateral accretion sets, a) & b) main channel, c) chute channel. Thickness measurements (top to bottom) 12.2, 8.62, 9.08 meters.

Clay-clast conglomerate

Intraformational clay-clast conglomerates are present stratigraphically above many major bounding surfaces throughout the MSSS (Figure 11). The clay clasts appear circular to oval and are up to one meter in diameter. They are composed of clay and other fine-grained deposits that have the same morphology as surrounding floodplain deposits.

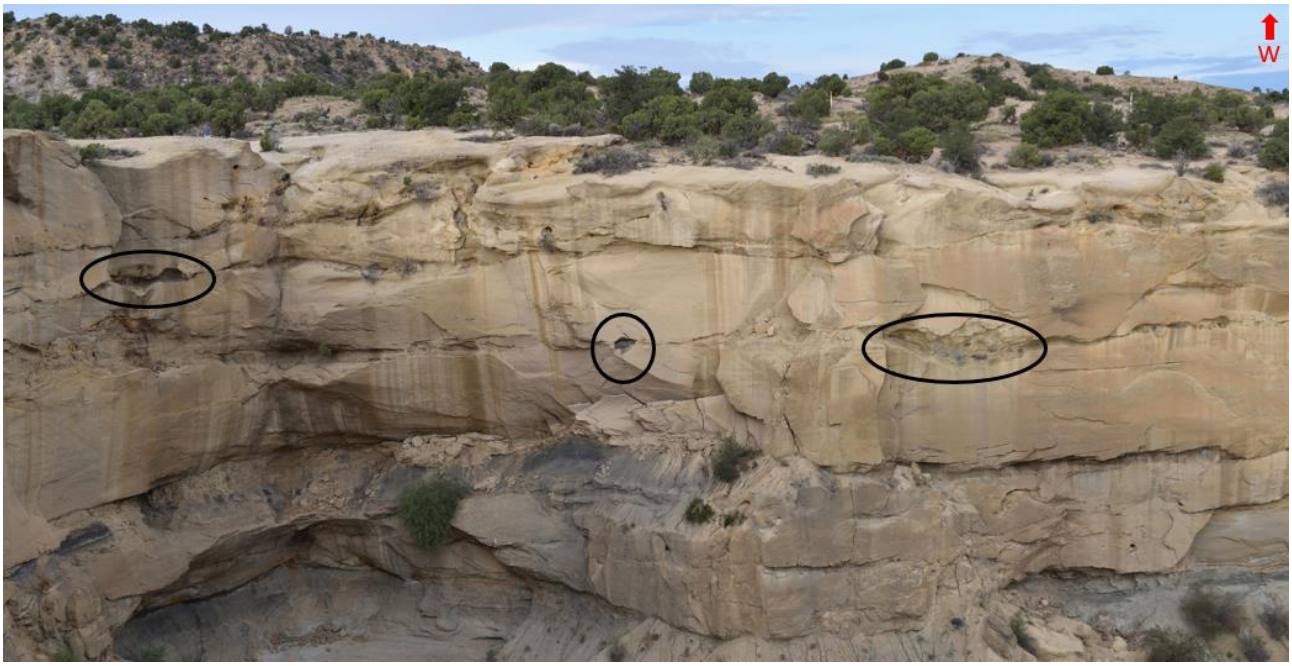

Figure 11. Deposits interpreted to be intraformational clay-clast conglomerates (black ovals).

Clay clasts are formed as highly turbulent water rips up fine-grained flood plain material and subsequently deposits them in the deepest part of the channel as lag deposits (Moraes and de Ros, 1992; Worden and Morad, 2003; Nichols, 2013). Clay clasts are preserved because clay is highly cohesive (Worden and Morad, 2003; Nichols, 2013).

Floodplain material and sandy overbank deposits

Only minor floodplain material and sandy overbank deposits are preserved within the MSSS. These deposits only outcrop in cliff faces and as a result, were not directly accessible. Floodplain material occurs in thinly laminated layers of clay to silt sized grains (Figure 12). Overbank deposits occur as thin lenses of sand contained within finer floodplain material (Figure 12). The area of these exposed facies in the MSSS is very minor compared to the area of exposed sandstone.

Figure 12. Sandy overbank deposits (blue arrow) encased in flood plain material.

Floodplain material is interpreted to be fine-grained sediments that slowly aggraded vertically along channel banks during bankfull events (Bridge, 2003). Deposition of sandy overbank deposits likely occurred during events that were larger than bankfull, in which water and coarser sediment prograded onto the floodplain. This tends to also occur along paleo-cutbanks of meandering rivers as crevasse splays (Slingerland and Smith, 2004).

Storeys

Five storeys were identified in the 3-D outcrop model and each storey is interpreted to represent separate channel-belts (Figure 13). Within each storey, other minor bounding surfaces are present that likely represents internal processes within a single channel-belt. These are indicated by pink and yellow lines in Figures 14 and A1; yellow represents internal aggradational surfaces, and pink represents internal erosional surfaces. Examples of internal process features in the

MSSS are displayed in Figure 15. Crossbedding was observed in all storeys of the MSSS. Vertical storey thickness calculations, standard deviations from the mean, and estimates of cannibalization are contained in Table 1. Estimates of the amount of cannibalization for each storey was calculated by finding the difference between measured maximum storey thicknesses and the mean lateral accretion set thickness (as a proxy for paleo depth) (Table 1). All storeys in the MSSS appear to be vertically truncated and in some places their thickness approaches zero (Table 1). Truncation appears to have occurred to each storey by the subsequent storey. Paleocurrent indicators were measured for all storeys, but the density of measurements increased with each storey up section, due to accessibility. Paleocurrent directions are listed in Table A3 and presented here by storey, as Rose diagrams (Figure 16).

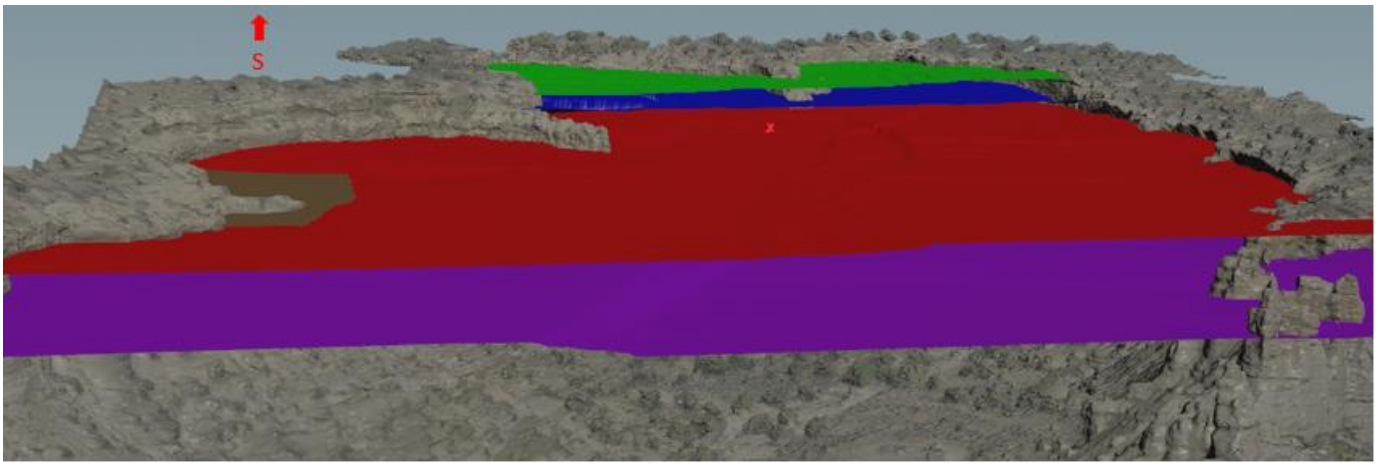

Figure 13. Five storey/channel-belt bases in 3-D outcrop model in Houdini From oldest to youngest, the bottom most storey is purple and will be referred to as storey A, brown is storey B. red is storey C, blue is storey D, and green is storey E.

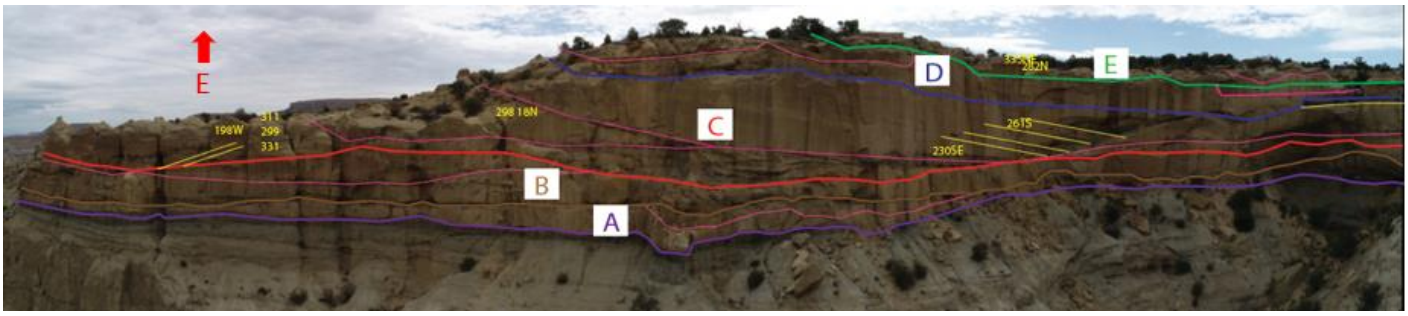

Figure 14. Bounding surfaces and paleo current measurements in Adobe Illustrator for far east wall only (all others can be found in Appendix Figure A1) and storeys are indicated by different color drafted lines and letters. Drafting surfaces: purple = base of storey A, brown = base of storey B, red= base of storey C, blue = base of storey D, green = base of storey E, pink = internal erosional surfaces, yellow = internal aggradational surfaces.

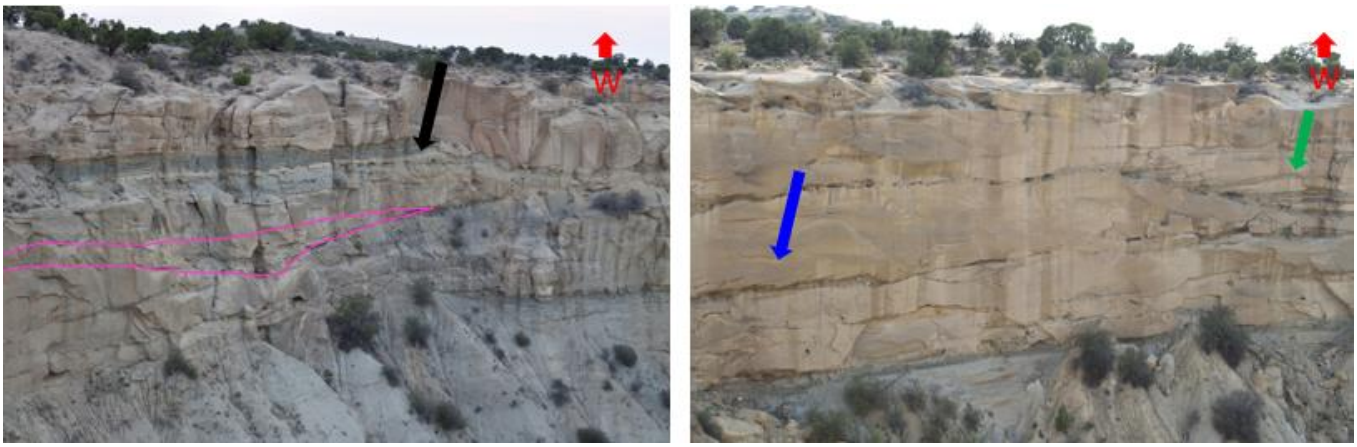

Figure 15. Internal features, pink lines are scour, black arrow indicates crevasse splay, blue arrow indicates lateral accretion sets of point bar, and green arrow indicates lateral accretion sets of point bar of chute channel.

Table 1. Storey geometries measured by raster calculator (performed in ArcMap) and lateral accretion set thicknesses as proxy for estimated initial storey thicknesses. Values rounded to the nearest hundredth. -- Calculations not applicable for storey because initial measured thickness is greater than estimated initial thickness.

Storey	Maximum vertical thickness (meters)	Estimated initial vertical thickness (meters)	Estimated cannibalization (meters)	Estimated percent cannibalized
A	4.83	8.62 - 12.2	3.79 - 7.37	44 - 60
B	6.45	8.62 - 12.2	2.17 - 5.75	25 - 47
C	13.05	8.62 - 12.2	--	--
D	2.53	8.62 - 12.2	6.09 - 9.67	71 - 79
E	6.06	8.62 - 12.2	2.56 - 6.14	30 - 50

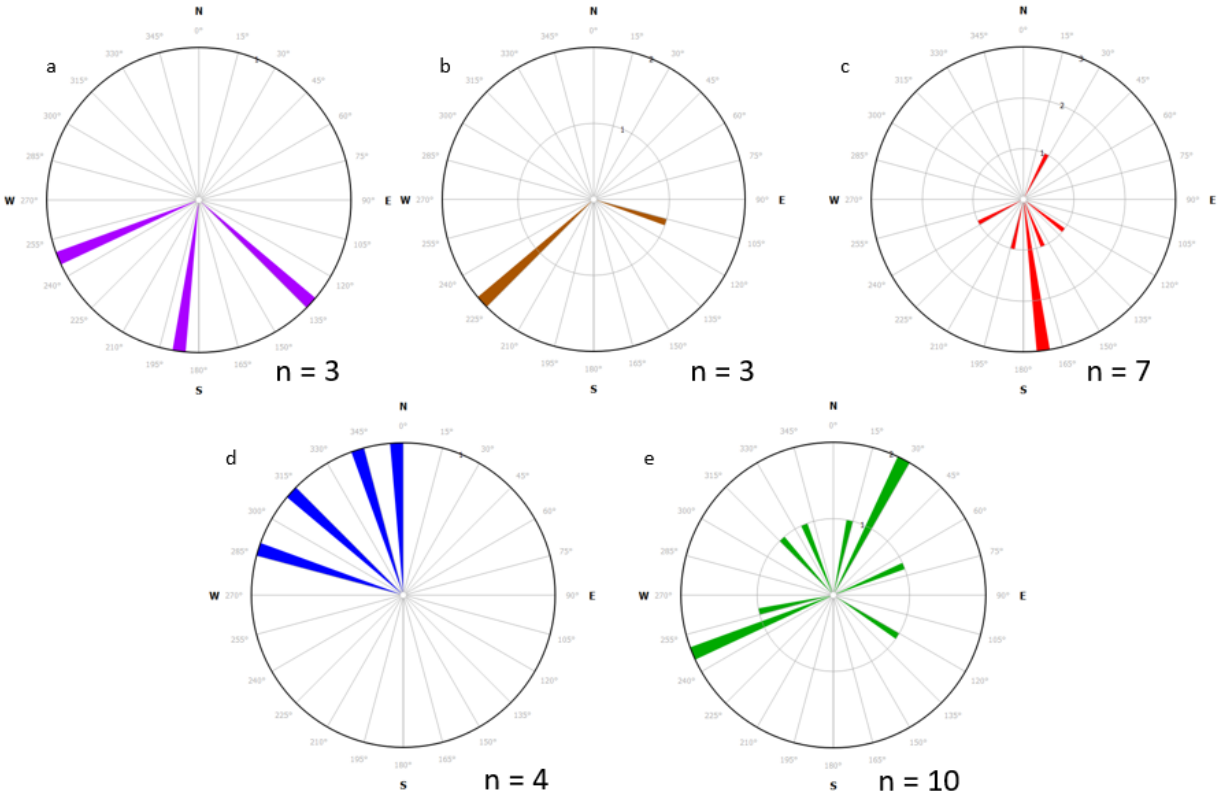

Figure 16. Rose diagrams for paleocurrent indicators by storey, a) storey A, b) storey B, c) storey C, d) storey D, e) storey E, and n = number of measurements.

Internal processes acted upon the storeys and are evidenced by point and compound bars, crevasse splays, scouring, reactivation surfaces, and laterally migrating chute channels. Point bar

deposits were found in storey C and compound bar deposits were found in storeys C, D, and E. A compound bar transitions vertically or laterally from crossbedding to plane bedding, without observable separation (Allen, 1983). Plane bedding can be produced by lower and higher flow regimes than crossbedding, therefore compound bars can represent fluctuations in river stage (Allen, 1983). Compound bars can also form as a result of changing sediment size (Allen, 1983) and sediment size is related to bar height (Bridge, 2003). It appears that modern erosion removed portions of the upper-most three storeys in the central and northern areas of the MSSS where their lateral extents appear to be truncated (Figure 17).

Figure 17. Erosional surface of west side MSSS, blue arrows indicate possible erosional surfaces of storeys C, D, and E.

Storey A

Storey A is the basal storey (indicated as purple basal bounding surfaces in Figures 14 and A1) of the MSSS, meaning that it was the first storey to be deposited. Storey A has an irregular lower bounding surface that rests atop floodplain material in all but one location, where there is a 63.1-meter-wide scour into lower sandstone (Figure 18a). Storey A only contains the channel-belt sandstone facies and paleo current measurements indicate a general paleo flow toward the south (Figure 16a). Lateral accretion deposits were not observed in this storey.

The deposits that sit stratigraphically below storey A, are interpreted to be of the Kutz member of the Nacimiento Formation (Figure 4).

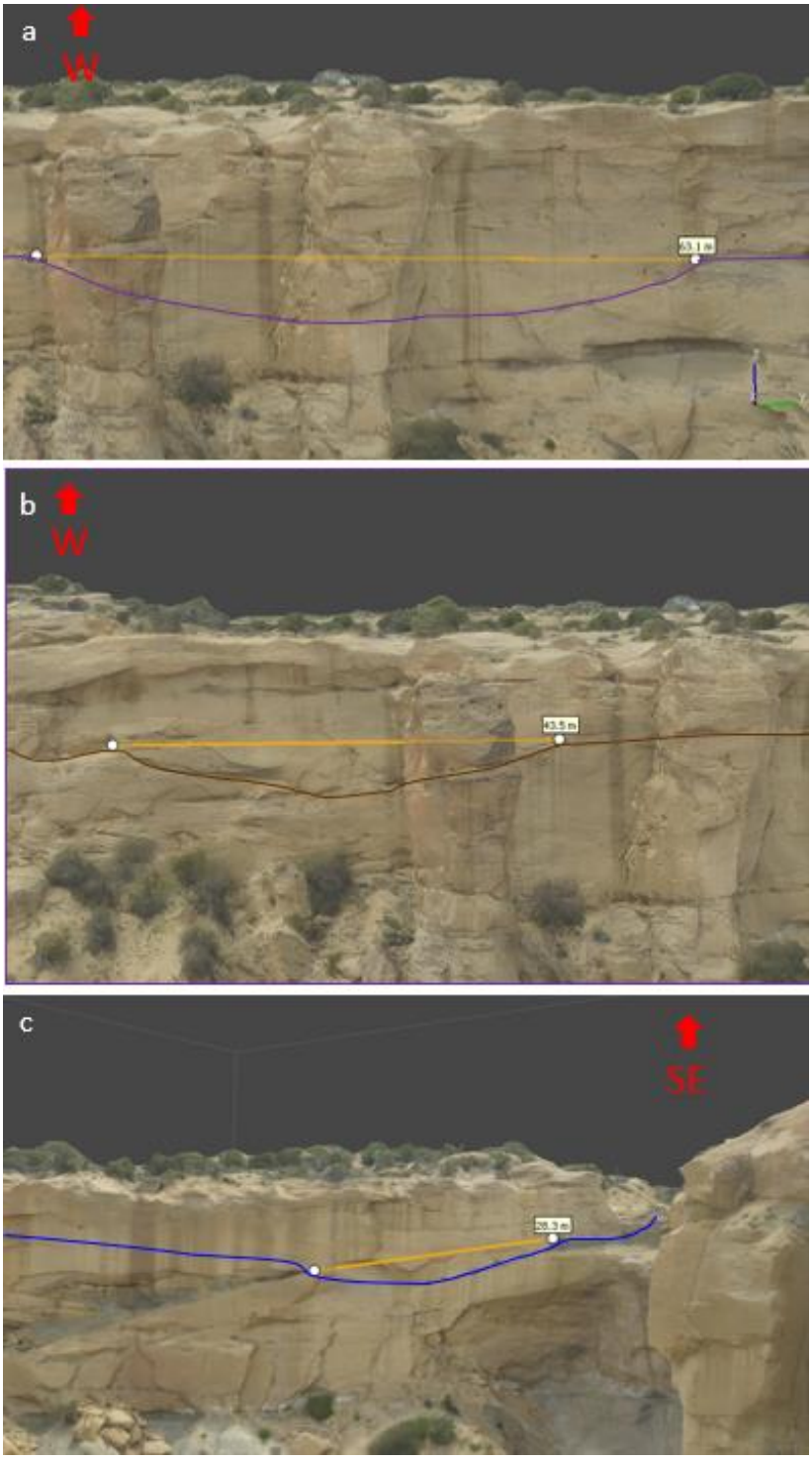

Figure 18. Bounding surfaces of storeys with scours, a) storey A (purple line), 63.1 m long (shown in orange), b) storey B (brown line), 43.5 m across, and c) storey D (blue line), 28.3 m across. Scour lengths were measured on 3-D outcrop model.

Storey B

The lower boundary of storey B (indicated as brown basal bounding surfaces in Figures 14 and A1) appears irregular and contains a 43.5-meter-wide scour into storey A below (Figure 18b). Storey B contains sandstone and a 6.5-meter covered interval that is interpreted to be floodplain material (Figure 19). Crossbedding in storey B indicates southwesterly paleoflow (Figure 16b). Lateral accretion deposits were not observed in this storey.

Figure 19. Two views of covered interval of floodplain material in story B, indicated with blue arrows, a) view looking west, and b) view looking southeast.

Storey C

Storey C has an irregular storey boundary (indicated as red basal bounding surfaces in Figures 14 & A1). Storey C contains sandstone facies and the largest amount of floodplain material and overbank deposits preserved in the MSSS. It also contains multiple lateral accretion sets, petrified log concretions in situ (Figure 20), and clay-clast conglomerates. Crossbedding measured in this storey suggested paleoflow was generally toward the south (Figure 16c). The lateral accretion sets of storey C indicate that paleocurrent was toward the northwest or southeast and petrified log concretions in storey C also indicate a paleocurrent toward the northwest or southeast (Figure 21).

Figure 20. Petrified log concretion in storey E.

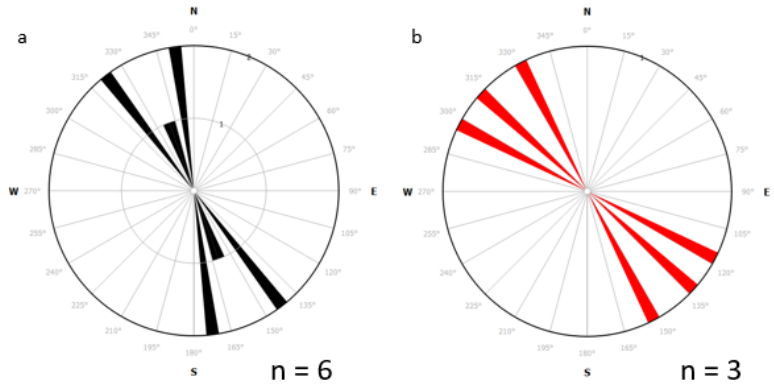

Figure 21. Rose diagrams of possible paleocurrent directions from storey C, a) petrified log concretions, b) lateral accretion sets.

This storey contains all lateral accretion sets that are observed in the MSSS. One set of lateral accretion terminates into inclined channel-belt sandstone and is thus interpreted to have been a migrating chute channel (Figure 22). By comparing paleocurrent directions of lateral accretion

sets (perpendicular to dip direction) and petrified log concretions (line bearing) with crossbedding directions for storey C, I determined that the dominant paleoflow was toward the south-southeast. Interbedding of floodplain material and overbank deposits in this storey appears to grade coarser towards the southwest and is interpreted to be a crevasse splay (Figure 23).

Figure 22. Chute channel lateral accretion sets terminating into inclined sandstone strata toward the south.

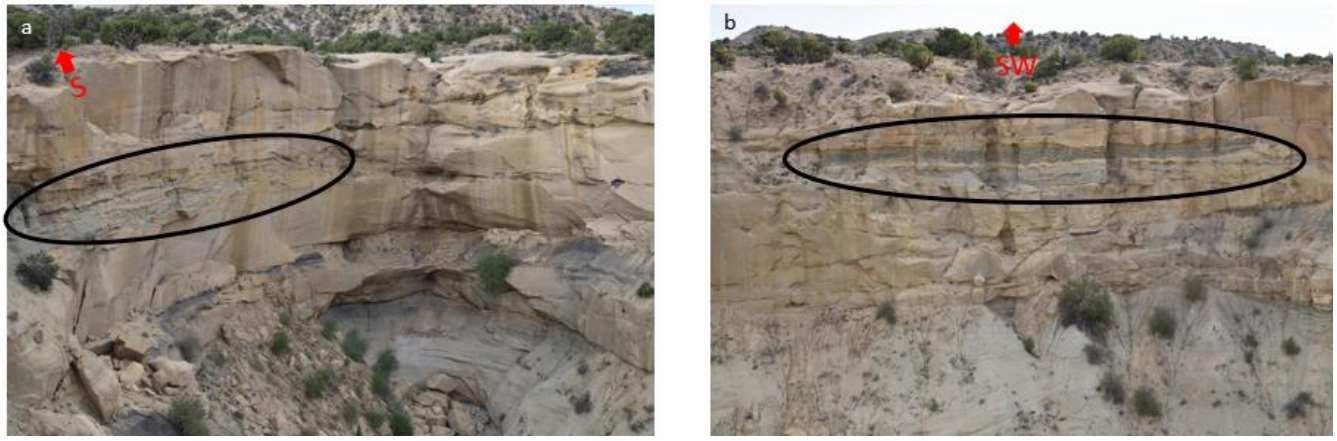

Figure 23. Black ovals show crevasse splay deposits in floodplain material of storey C, a) and b) are different views of the same deposits.

Storey D

The lower boundary of storey D (indicated as blue bounding surfaces in Figures 14 and A1) is irregular and contains a 28.3-meter-wide scour into storey C (Figure 18c). The lower bounding surface is the most irregular of all the channel-belts as indicated by the highest standard deviation of 3.51 meters from its mean elevation (Table 1). Storey D contains channel-belt sandstone and clay-clast conglomerates. Crossbedding in this storey indicate a northwesterly paleocurrent (Figure 16d). It appears that modern erosion truncated this storey, so the full lateral extent of this storey is no longer preserved (Figure 17).

Storey E

The bounding surface storey E (indicated as green bounding surfaces in Figures 14 and A1) has an irregular boundary with storey D (irregular bounding surface) and is the youngest storey that is preserved within the MSSS. It contains channel-belt sandstone, petrified log concretions, clay-clast conglomerates, and this storey covers the smallest geographic area of the MSSS since much of this storey was eroded under more modern conditions. Storey E is the uppermost storey and it makes the topography in the southern portion of the MSSS, so many bar forms with plane bedding and planar and trough crossbedding are readily observed and easily measured (Figure 25). Crossbedding in storey E indicates a general flow direction toward the northeast but varied widely (Figure 16e), while the orientations of the petrified log concretions varied widely (Figure 24). Lateral accretion deposits were not observed in this storey.

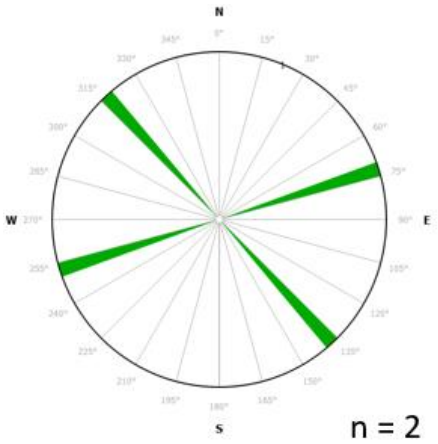

Figure 24. Rose diagram for possible paleocurrents for petrified log concretions in storey E.

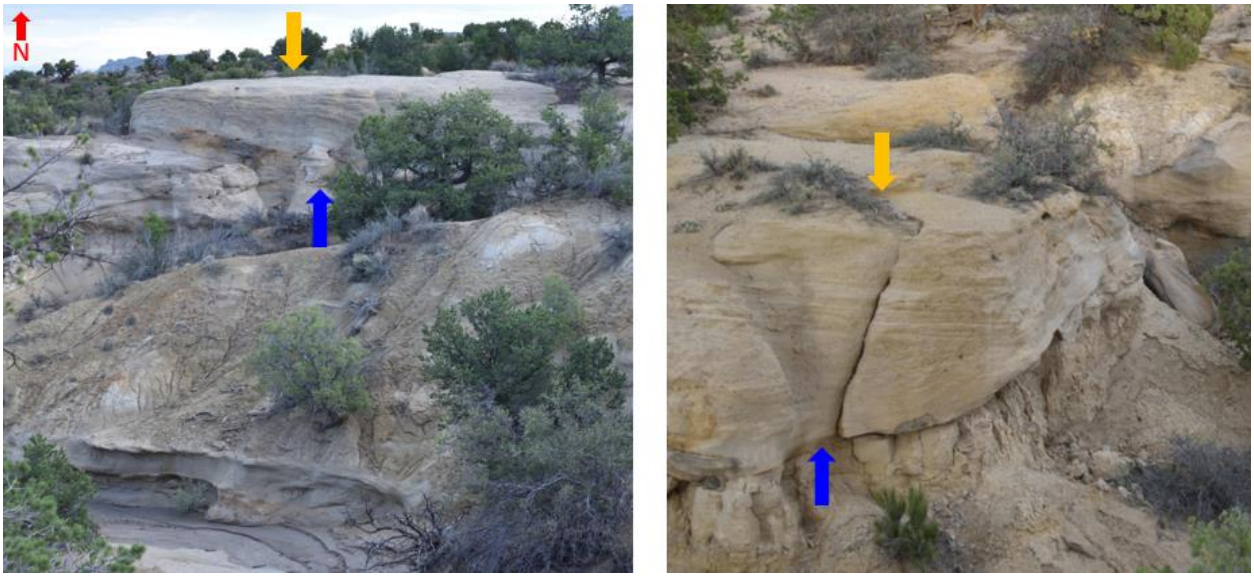

Figure 25. compound bar deposits in storey E, blue arrows indicate crossbedding (bottoms) and orange arrows indicate plane bedding (tops).

Storey E contains the highest variability in paleocurrent measurements (Figures 16e & 24), and that is easily observed in outcrop because it is the uppermost storey, an example is Figure 26. Many bar forms are exposed in this storey and sedimentary structures suggest they are mid-channel bar forms, and many appear to be compound bars (Figure 25) (Allen, 1983). The limited extent of this storey is assumed to have been lost in large part due to Miocene and recent erosion (Figure 17).

Figure 26. Examples of variability in crossbedding directions observed in storey E.

Storey edges

The sand bodies in the MSSS experienced a high degree of sand amalgamation and the edges of storeys are not present within the MSSS detailed study area. Observations of non-eroded edges could only be made outside of the MSSS detailed study area, within other nearby outcrops of the Angel Peak member. Storey edges were located and imaged in the field, located in Google Earth, and approximate storey base elevations were compared to 3-D outcrop model elevations. Storey edges for A were located approximately 660 meters east of the MSSS detailed study area, and storey edges for B and E were located approximately 650 meters west of the MSSS detailed study area (Figure 5). The edges of storey A are characterized as erosional and sawtooth (Figures 6 & 27a). The visible edge of storey B is sawtooth, and the edges of storey E are steep-sided and sawtooth (Figure 6 & 27b). All observed storey edges are separated by floodplain material. Due to the limited extent of the MSSS detailed study area, W/Ts could not be measured for the storeys.

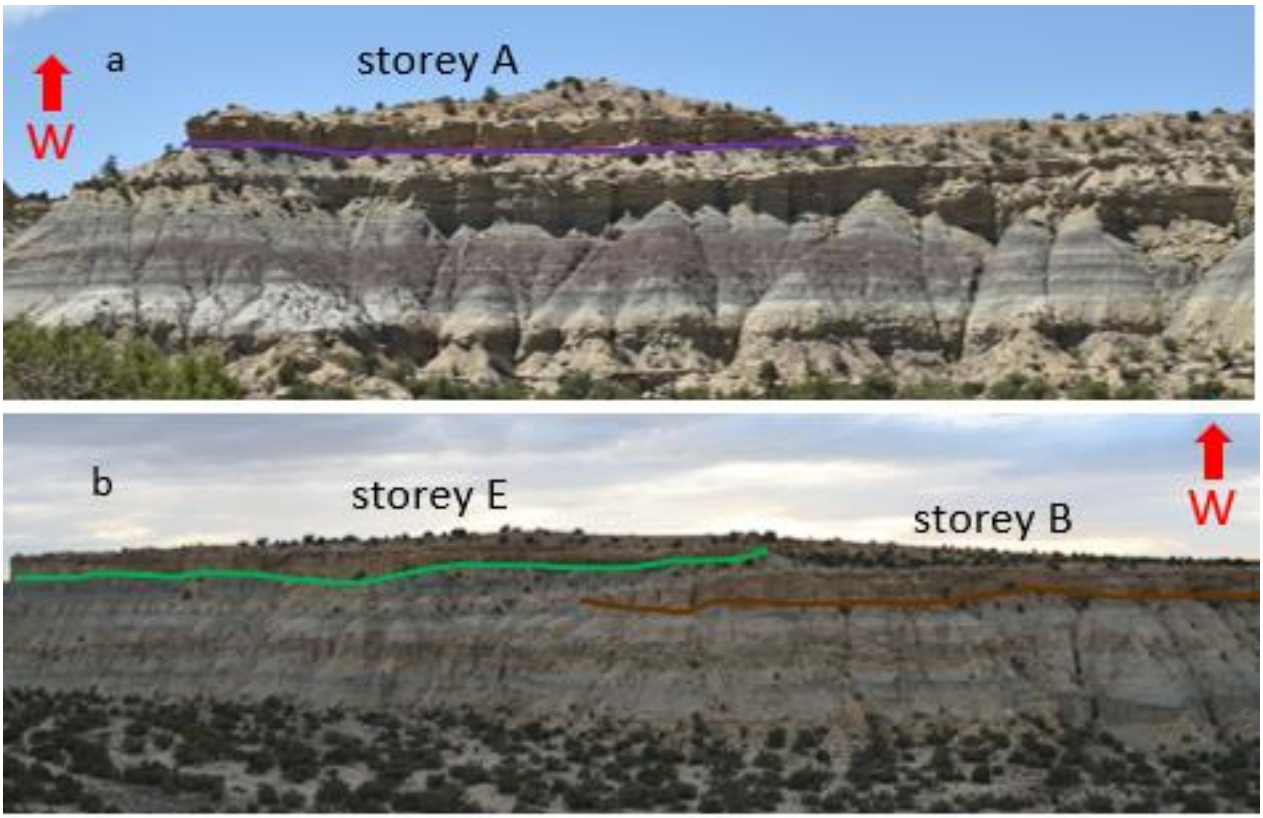

Figure 27. Storey edges located outside of the MSSS, a) storey edges of B (sawtooth) and E (steep-sided and erosional), located 650 meters toward the west and b) storey edge of A (erosional and sawtooth), located 660 meters toward the east.

MSSS

The lower bounding surface of the MSSS is the same bounding surface as storey A, the first storey of the MSSS. Overall, the sheet bounding surface appears to be smooth (Figure 28), with the exception of a localized large scour (Figure 18a). The estimated vertical cannibalization that occurred in each storey was determined by subtracting maximum storey thickness from lateral accretion thickness and it ranges from less than one meter to almost four meters (Table 1). The estimated amount lost ranges from 10 to 44 percent (Table 1). The local measurements of paleo current in the MSSS suggest that paleoflow was to the southwest during deposition of storeys A, B, and C. During deposition of storey D, the paleo flow shifted toward the northeast, and finally during deposition of storey E paleo flow was generally toward the north (Figures 16, 21, 24, & 29). Moving up section, as the storeys become younger, paleocurrent measurements and

observed crossbedding of surficial bars appear to become more disparate (Figure 16e, 25, & 26). These are measurements and observations from a discrete location of a DFS and may not reflect overall/main channel paleocurrent directions. There are many reactivation surfaces and indurated layers in the MSSS, and they appear to increase in abundance moving up section. The indurated layers also appear to become more iron-stained and a larger number of concretions are observed moving up section.

Figure 28. Smooth basal bounding surface of storey A (and MSSS) on floodplain deposits of Main Body member (blue arrow).

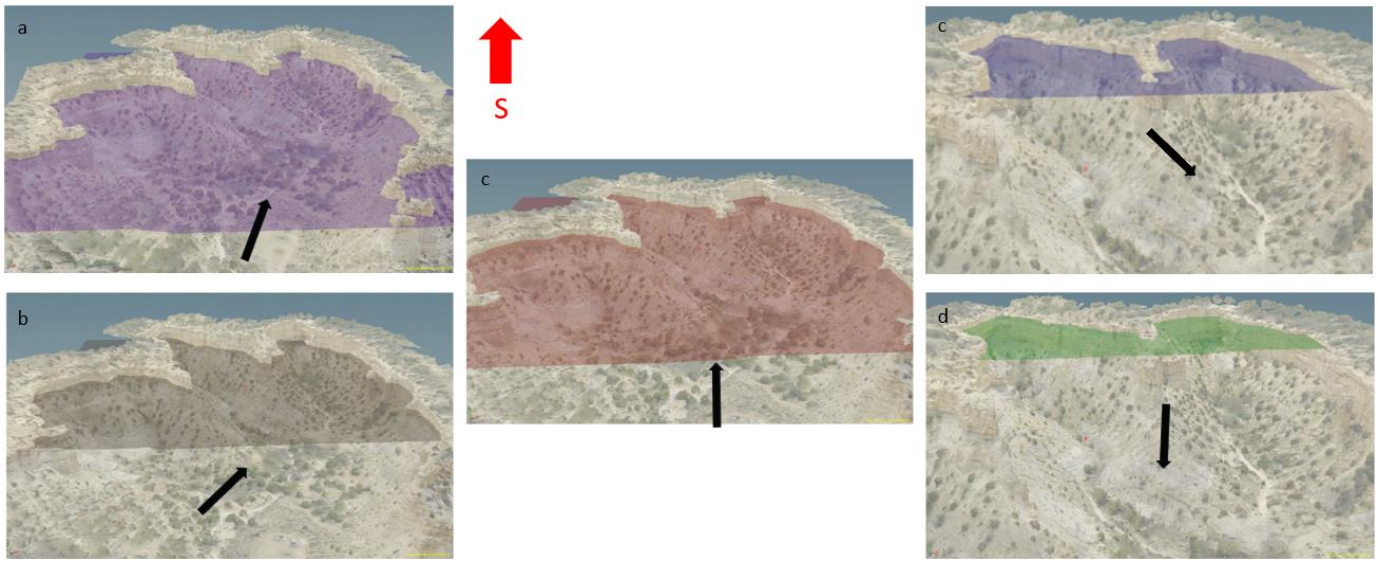

Figure 29. Interpolated bounding surfaces in 3-D outcrop model for storeys A, B, C, D, and E. Black arrows indicate approximate paleo flow directions.

There are only minor amounts of floodplain material and overbank deposits preserved in the MSSS. This is likely because after each avulsion there was a high degree of sediment reworking (Kjemperud, et al., 2008; Benhallam et al., 2016). Floodplain material and overbank deposits aggraded during bankfull events with each storey but were later removed by cannibalization of the subsequent storey (Gibling, 2006). The degree of vertical truncation observed in the MSSS appears to be relatively consistent in all storeys. The topography that remains of the MSSS suggests that portions of storeys C, D, and most of E were removed by erosion beginning in the Miocene and likely continuing into the recent (Braschayko, 2008; Cather, 2012).

DISCUSSION

Results of this study indicate that MSSS in the detailed study area amalgamated through a combination of processes. The major bounding surfaces of the MSSS and the storeys they comprise represent the amalgamation of discrete channel-belts. Other minor bounding surfaces were identified and correlated to internal processes within each channel-belt. The degree of

vertical truncation in each channel-belt and high net-to-gross ratios suggests that there were intervals of zero aggradation and/or erosion (scouring, induration, or reactivation surfaces) which occurred throughout deposition of the MSSS, but appear to increase with each successive storey.

Avulsion and reoccupation processes

The stacked nature of the channel-belt deposits and the absence of channel-belt edges in the MSSS suggests that avulsion and reoccupation of channel-belts occurred in a clustered style during deposition. This occurred a minimum of five times to produce the MSSS. Additional support of channel-belt stacking includes an irregular sheet bounding surface, clay-clast conglomerates in three of the storeys (C, D, and E), and floodplain material in storeys B and C (e.g., Holbrook, 2000; Chamberlin and Hajek, 2015; Chamberlain, 2016). Most storey edges that were observed were characterized as sawtooth and all storey edges are separated by floodplain material. These findings confirm that these are distinct and separate, vertically-stacked channel-belts.

Each successive avulsion placed the river in nearly the same location within the central portion of the SJB to produce a five storey MSSS. Internal processes produced accretionary and erosional surfaces within each storey. The data collected for paleocurrent analysis indicates that the flow was toward the south and southwest but began shifting north during deposition of storeys D and E. This is consistent with uplifted sediment sources located just north of the basin (La Plata and San Juan uplifts) (Cather, 2004). However, a recently published study by Cather et al. (2019) found paleo flow currents for this member to be toward the east, which does not agree with general paleocurrent measurements found in this study. Cather et al. (2019) collected paleo current measurements (n = 100) from three different areas located three to six kilometers southwest of the MSSS. All three of their locations had dominant paleo currents toward the east

and are further up in section and stratigraphically above the MSSS (they are at higher elevations and dip has been reported as negligible for this part of the basin) (Carritt, 2014; Cather et al., 2019). It is possible that a later avulsion brought the river(s) back, and that river flowed toward the east (Cather et al., 2019). Another cause for different paleocurrent directions may be simply due to the small extent and local position of the MSSS in the SJB. It may not adequately represent paleocurrent for the entire Angel Peak member.

Internal processes

Storeys in the MSSS show evidence for migrating channels, flooding, and erosion. Channel migrations are observed in the MSSS and include lateral and vertical accretion as crossbedding, planar bedding, plane beds, and lateral accretion sets. Small scours and reactivation surfaces formed when ratios of discharge to sediment supply were high, while accretionary features such as bedding formed when these ratios were low. These surfaces are preserved in the rock record as crossbedding, planar bedding, lateral accretion sets, scours, and reactivation surfaces.

Flooding is evidenced by vertical accretion of floodplain material and overbank deposits preserved in storeys B and C. The presence of point bar deposits and crossbedding indicates that accretion did occur laterally, while the presence of floodplain material and compound bars deposits indicates that there was also vertical accretion occurring. Considering the appearance of fining upward deposits in the compound bars, it indicates that they likely formed during a falling river stage. Also, wide variations in crossbedding directions can occur when river stage is falling because bar tops are dissected by divergent flows (Chakraborty, 1999). When a bar is exposed to the air it can become indurated and may become a reactivation surface. The combination of these features suggest that during deposition of storeys C, D, and E, there were large fluctuations to river stage and discharge.

Lateral accretion sets and a high degree of sand amalgamation are consistent with deposition by a meandering river in the medial to proximal transition zone of a DFS in the SJB during the Paleocene (Williamson, 1993; Hobbs, 2016). Lateral accretion set thickness in the MSSS are analogous to paleo channel depths that were approximately eight to twelve meters. There is no evidence of abandoned channels, scroll bar topography, or apparent point bar overprinting in the MSSS, and thus it does not appear that the residence time for each channel-belt was adequate for complex meanders to form or significant overprinting to have occurred.

Despite one channel-belt edge characterized as steep-sided, data collected and interpreted for this study does not indicate that amalgamation occurred by an incised valley process. Formation of incised valleys has been strongly linked to climate changes and base level changes (Weissmann et al., 2002; Fontana et al., 2004; Gibling et al., 2005; Nichols, 2015). Recent research has shown that climate change was not occurring during this time (Hobbs, 2016) and the SJB may have been too far inland to feel effects of marine base level.

Depositional history of MSSS

Each channel-belt experienced some degree of vertical truncation, which suggests that cannibalization occurred between and/or throughout deposition. If we assume lateral accretion thickness as a proxy for vertical storey thickness (Table 1) (Nichols, 2013), then the average vertical thickness (and bankfull stage) would be the average lateral accretion set thickness. Using this logic, a couple more assumptions can be made. First, the amount of vertical cannibalization that occurred in each channel-belt is equal to the difference between vertical storey thickness and measured maximum storey thicknesses and these amounts vary by approximately three to six meters (Table 1). Second, with a deposition rate of 0.19mm/yr (Carritt, 2014) and average storey thickness of 8.62 to 12.2 meters, the return interval for

channel-belts would be approximately every 45 to 64 thousand years, which exceeds Carritt's avulsion interval estimate of every 34 thousand years (2014) by at least 11 thousand years. If approached alternatively and we assume a deposition rate of 0.19mm/yr for 34 thousand years, then each channel-belt thickness should be approximately 6.5 meters. The latter would infer that far less cannibalization occurred to the channel-belts and it is also far less than some of the measured maximum storey thicknesses (Table 1). It is therefore reasonable to assume that the return intervals for avulsions of channel-belt occurred closer to every 45 thousand years during this time. An interval of 45 thousand years is more consistent with measured vertical thicknesses of the storeys and the degree of amalgamation that is observed. This is likely because Carritt's study involved a larger succession of the Nacimiento formation in Kutz Canyon and it was lower in the section, when accommodation space in the SJB was assumed to be much greater (2014).

No evidence exists for changes to basin subsidence occurring in the SJB during deposition of the MSSS (Cather, 2004). A small amount of localized subsidence may have occurred to isolated aggrading areas, where aggradation created local subsidence which attracted channel-belts back to this location on the DFS (Hofman et al., 2011; Chamberlin and Hajek, 2015). According to Slingerland and Smith (2004), avulsion by annexation is the reoccupation of channel-belts to the same location on the floodplain as previous channel-belts. This is common in fluvial literature and it is thought play a role in modern avulsions (). If the channel-belt returned approximately every 45 to 64 thousand years, the full depositional interval of the MSSS would be approximately 225 to 340 thousand years, which is appropriate for channel-belt clustering (Hofman et al., 2011). Although Williamson (1993) did not report the depositional time interval for the Angel Peak member, he did place it (unnamed member) stratigraphically equal to the upper half of the Ojo Encino member further north in the basin. Deposition of the Ojo Encino

member occurred throughout the normal and reversed polarity of chron 27 (Williamson, 1993). If we assume that the Angel Peak member comprised the first half of chron 27 and use the most recent magnetic polarity in the SJB of Leslie et al. (2018), the deposition interval for the first half of chron 27 would be approximately 340 thousand years. This would provide a return interval for channel-belts to be approximately every 68 thousand years, which is very close to the upper range of estimates for this study.

The MSSS contains only small amounts of preserved fine-grained material, a large degree of sand amalgamation, cannibalization, scour deposits, and a high net-to-gross ratio. These phenomena are indicative of relatively low aggradation rates, diminishing accommodation space, and increased channel-belt clustering in the basin (Mackey, et al., 1995; Kjemperud et al., 2008; Benhallam et al., 2016). Aslan and Blum (1999) found a relationship between avulsion by annexation and low rates of aggradation in the Texas River. This is consistent with other findings, that the Nacimiento Formation was deposited in the proximal to medial transition zone of a prograding DFS as accommodation space was diminishing (Williamsom, 1993; Weissmann et al., 2013; Hobbs, 2016; Leslie et al., 2018; Cather et al., 2019).

The modern topography of the MSSS is a result of erosion that has occurred over the last 15 million years (Braschayko, 2008; Cather, 2012). Erosion also likely removed several channel-belt edges of the Angel Peak member in the Angel Peak area.

CONCLUSIONS

Fluvial outcrop studies of terrestrial basins are vital to our understanding of compartmentalization in aquifer systems. New photogrammetric techniques and 3-D outcrop model studies allow the identification and accurate correlation of bounding surfaces in a multi-

storey sheet sandstone on outcrops that are complex in form. This provides accurate correlations across discontinuous areas and around corners where it may not be possible or very difficult otherwise.

The fluvial deposits of the MSSS were created by both internal processes of a channel-belt (H1) and avulsion and reoccupation of channel-belts (H2), by a meandering river during the Paleocene. Evidence suggests that internal processes such as channel migrations and scouring, were active during deposition of each storey. Avulsion and reoccupation of channel-belts occurred to produce the five storeys of the MSSS in the detailed study area. Low available accommodation space in the SJB is consistent with increasing geomorphic base level in the basin. This caused erosion to occur more proximally in the channel-belt, which helped provide sediment for further downstream to the MSSS.

The channel-belts amalgamated in a clustered style in the proximal to medial transition zone of a DFS. This was during a time of limited aggradation because of limited space, likely returning on average every 45 to 64 thousand years back to the same location, a result of avulsion by annexation (Slingerland and Smith, 2004). Between avulsion intervals, the channel-belts had enough time to vertically and laterally aggrade and likely cannibalize large portions of the previous channel-belts deposits. The resultant architecture of the MSSS is a highly amalgamated succession with high net-to-gross ratios and very little floodplain material or overbank deposits preserved.

The MSSS of the Angel Peak member contains a large amount of sand and very little fine-grain material, which would make it an ideal reservoir. However, the cannibalization that appears to have occurred to the MSSS truncated each storey vertically, essentially reducing the amount of channel sands that were preserved in each storey. In addition, the MSSS contains many

bounding surfaces that have silt, mud, or clay sized grains that disrupt sandstone connectedness, therefore all of them have the potential to disrupt fluid flow in the subsurface.

LIST OF APPENDICES

APPENDIX I

Table A1. Camera types for photo acquisition for the MSSS.

Camera type	Lens type	Resolution
Gimbaled UAS- Phantom 4	FOV 94° (20 mm) (35 mm format equivalent)	12 megapixels
Nikon D700 digital SLR	28-50 mm, 105 mm, and 300 mm	12 megapixels
Multispectral NIR- MAPIR 3W	87° HFOV (19 mm)	12 megapixels
Nikon D5600 digital SLR	18-55 mm	14 megapixels

Table A2. Agisoft Photoscan image processing parameters.

Photoscan model processing parameters		
	Planview	**Vertical cliffs**
Dense point cloud	Quality: High	Quality: High
	Depth filtering: Mild	Depth filtering: Mild
Mesh	Surface type: Height field (2.5D)	Surface type: Arbitrary (3D)
	Source data: Dense cloud	Source data: Dense cloud
	Face count: High (37,579,915)	Face count: High (22,422,719)
Texture	Mapping mode: Keep uv	Mapping mode: Keep uv
	Blending mode: Mosaic	Blending mode: Mosaic
	Texture size: 8192	Texture size: 8192

Photoscan shifts for export		
X (m)	**Y** (m)	**Z** (m)
243,300	4,051,200	1950

Table A3. Paleocurrent measurements used for Rose diagrams, by storey.

Storey E				
Strike/ bearing azimuth	Dip Direction	Paleocurrent indicator	Dip azimuth	Alternate azimuth
335	northeast	crossbedding	65	
282	north	crossbedding	12	
335	southwest	crossbedding	245	
345	west	crossbedding	255	
337	south	crossbedding	247	
245	northwest	crossbedding	335	
225	northwest	crossbedding	315	
297	northeast	crossbedding	27	

296	northeast	crossbedding	26	
89	west	crossbedding	doesn't work, not used	
31	east	crossbedding	121	
315		petrified log concretion	315	135
72		petrified log concretion		252
Storey D				
220	northwest	crossbedding	310	
250	northwest	crossbedding	340	
198	west	crossbedding	288	
268	north	crossbedding	358	
Storey C				
298	north	crossbedding	28	
217	southeast	crossbedding	127	
280	south	crossbedding	190	
245	southeast	crossbedding	155	
84	south	crossbedding	174	
330	southwest	crossbedding	240	
352		U	172	
254	north	petrified log concretion	344	164
230	northwest	petrified log concretion	320	140
245	southeast	LAS	335	155
230	southeast	LAS	320	140
261	south	LAS	351	171
262	south	LAS	352	172
311		crossbedding	131	
299		crossbedding	119	
331		crossbedding	151	
Storey B				
198	east	crossbedding	108	
186	west	crossbedding	225	
315	southwest	crossbedding	225	
Storey A				
42	southeast	crossbedding	132	
158	west	crossbedding	248	
275	south	crossbedding	185	

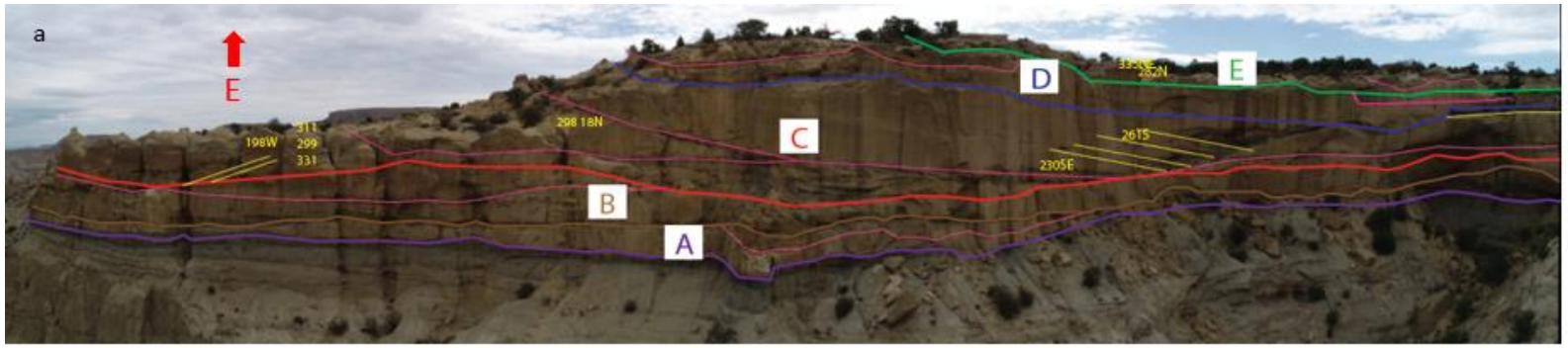
a
E
198W
311
299
331
298 18N
C
D
E
2615
2305E
B
A

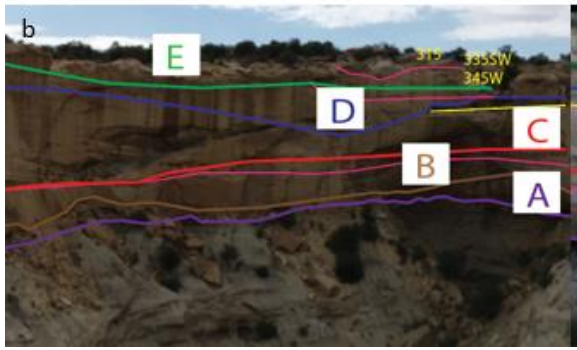
b
E
D
C
B
A
345W

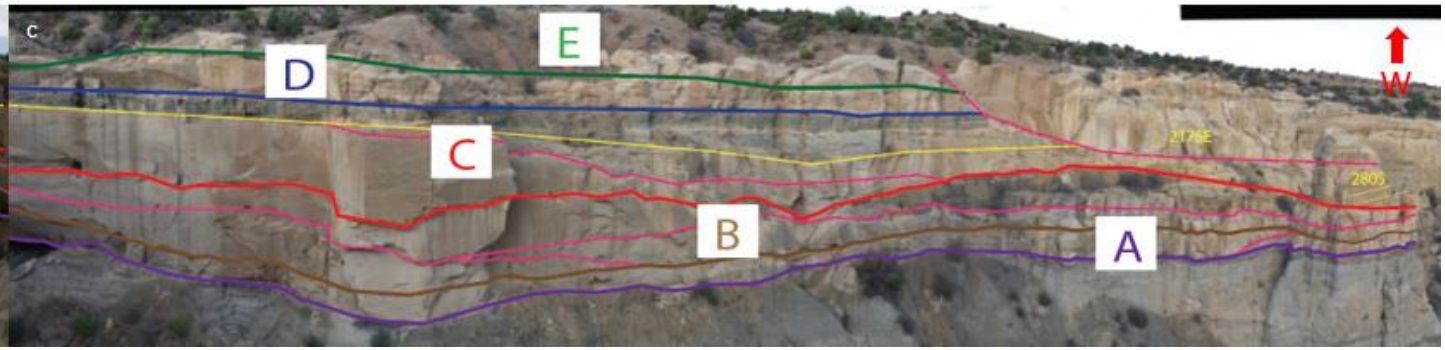
c
E
D
C
B
A
W
2176E
2805

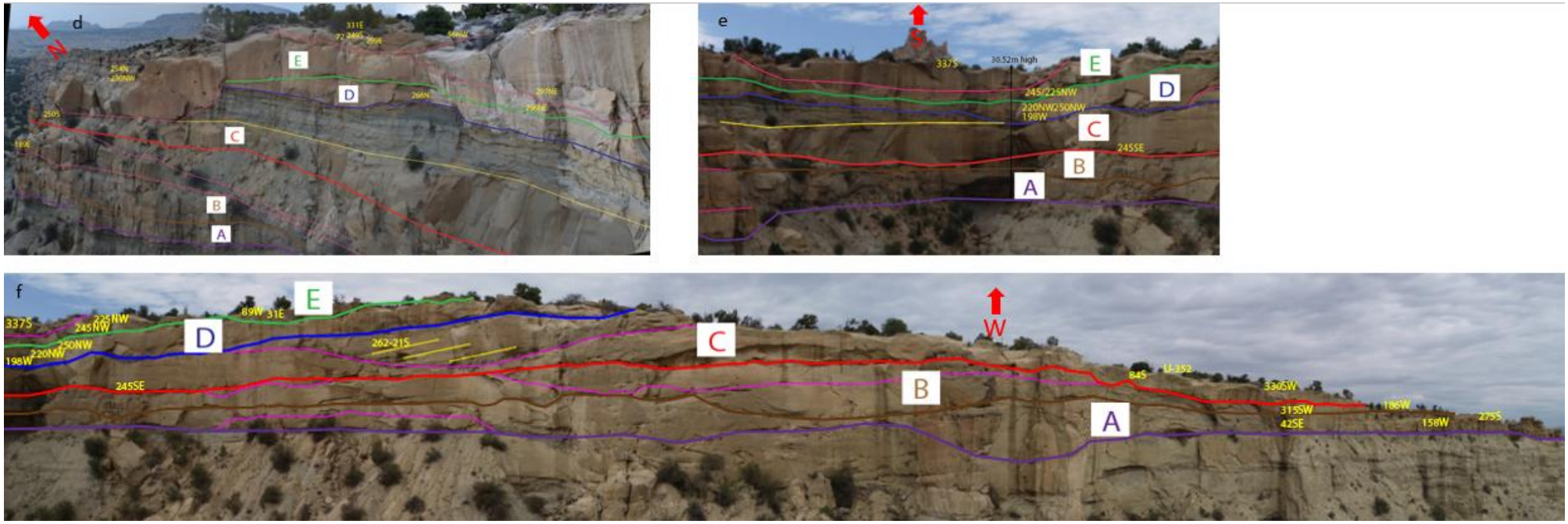

Figure A1, Bounding surfaces and paleo current measurements in Adobe Illustrator and storeys are indicated by different color drafted lines and letters. Drafting surfaces: purple = base of storey A, brown = base of storey B, red= base of storey C, blue = base of storey D, green = base of storey F, pink = internal erosional surfaces, yellow = internal aggradational surfaces. a) through f) are views of MSSS starting from the furthest northeast (a) and ending the furthest northwest (f).

REFERENCES

Allen, J.R.L., 1968, Current ripples: their relation to patterns of water and sediment motion: Amsterdam, North-Holland.

Allen, J.R.L., 1983, Studies in fluviatile sedimentation: bars, bar-complexes and sandstone sheets (low-sinuosity braided streams) in the Brownstones (L. Devonian), Welsh Borders, Sedimentary Geology, 33(4), pp.237-293.Aslan, A. and Blum, M.D., 1999, Contrasting styles of Holocene avulsion, Texas Gulf coastal plain, USA, Fluvial sedimentology VI, 28, pp.193-209.

Baltz, E.H., 1967, Stratigraphy and regional tectonic implications of part of Upper Cretaceous and Tertiary rocks, East-Central San Juan Basin, New Mexico: USGS Prof. Paper 552, 101 p.

Benhallam, W., Turner, A., Stright, L., Johnson, C. L., 2016, Spatial analysis of channel-belt stacking patterns: metrics to discriminate between local and regional controls on deposition in the fluvial John Henry member of the Straight Cliffs Formation, Southern Utah, USA, Journal of Sedimentary Research, 86(11), 1310-1327.

Blakey, R.C. and Ranney, W.D., 2018, Flat-Slab Subduction, the Laramide Orogeny, Uplift of the Colorado Plateau and Rocky Mountains: Paleocene and Eocene: Ca. 65–35 Ma. In Ancient Landscapes of Western North America, pp. 131-148, Springer, Cham.

Bordy, E.M., Hancox, P.J., Rubidge, B.S., 2004, Fluvial style variations in the Late Triassic–Early Jurassic Elliot Formation, main Karoo Basin, South Africa. Journal of African Earth Sciences, 38(4), pp.383-400.

Braschayko, S., Kelley, S.A., Stockli, D., 2008, Exhumation history of the San Juan Basin: New Mexico Geology, v. 30, p. 56.

Bridge, J.S., 2003. Rivers and Floodplains: Oxford, U.K., Blackwell, 491 p.

Bull, W.B., 1991, Geomorphic Responses to Climatic Change. Oxford University Press, Oxford, 326 pp.

Carritt, J., 2014, Characterization of fluvial facies distributions and cyclicity using terrestrial lidar: Paleocene Nacimiento Formation, Kutz Canyon, New Mexico [thesis].

Cather, S.M., 2004, Laramide orogeny in central and northern New Mexico and southern Colorado, in Mack, G.H., and Giles, K.A., eds., The Geology of New Mexico: A Geologic History: New Mexico Geological Society Special Publication 11, p. 203-248.

Cather, S.M., Chapin, C.E., and Kelley, S.A., 2012, Diachronous episodes of Cenozoic erosion in southwestern North America and their relationship to surface uplift, paleoclimate, paleodrainage, and paleoaltimetry: Geosphere, v. 8, p. 1177-1206.Cather, S.M., Connell, S.D., Chamberlin, R.M., McIntosh, W.C., Jones, G.E., Potochnik, A.R., Lucas, S.G., and Johnson, P.S., 2008, The Chuska erg: Paleogeomorphic and paleoclimatic implications of an Oligocene sand sea on the Colorado Plateau: GSA Bulletin, v. 120, p. 13-33.

Cather, S.M., Heizler, M.T., and Williamson, T.E., 2019, Laramide fluvial evolution of the San Juan Basin, New Mexico and Colorado: Paleocurrent and detrital-sanidine age constraints from the Paleocene Nacimiento and Animas formations: Geosphere, v. 15, p. 1–24, doi:10.1130/ges02072.1.

Chakraborty, T., 1999, Reconstruction of Fluvial Bars from the Proterozoic Mancheral Quartzite, Pranhita-Godavari Valley, India, in Fluvial Sedimentology VI, p. 451–466, doi:10.1002/9781444304213.ch31.

Chamberlin, E.P., Hajek, E.A., 2015, Interpreting paleo-avulsion dynamics from multistory sand bodies, Journal of Sedimentary Research, 85(2), pp.82-94.

Chamberlin, E. P., 2016, Using fluvial stratigraphic architecture to isolate the role of avulsion processes in alluvial-basin filling (Order No. 10296948). Available from ProQuest Dissertations & Theses Global. (1847568764). Retrieved from http://libproxy.unm.edu/login?url=https://search-proquest-com.libproxy.unm.edu/docview/1847568764?accountid=14613

Davies, N.S., Gibling, M.R., 2010, Paleozoic vegetation and the Siluro-Devonian rise of fluvial lateral accretion sets, Geology; 38 (1): 51–54, doi: https://doi.org/10.1130/G30443.1

Donahue, M. M. S., 2016, Episodic uplift of the Rocky Mountains: Evidence from U-pb detrital zircon geochronology and low-temperature thermochronology with a chapter on using mobile technology for geoscience education (Order No. 10125719). Available from Dissertations & Theses @ University of New Mexico; ProQuest Dissertations & Theses Global. (1808233623). Retrieved from http://libproxy.unm.edu/login?url=https://search-proquest-com.libproxy.unm.edu/docview/1808233623?accountid=14613

Doyle, J.D., Sweet, M.L., 1995, Three-dimensional distribution of lithofacies, bounding surfaces, porosity, and permeability in a fluvial sandstone--Gypsy Sandstone of Northern Oklahoma, AAPG bulletin, 79(1), pp.70-95.

Durkin, P.R., Boyd, R.L., Hubbard, S.M., Shultz, A.W., and Blum, M.D., 2017, Three-Dimensional Reconstruction of Meander-Belt Evolution, Cretaceous McMurray Formation, Alberta Foreland Basin, Canada: Journal of Sedimentary Research, v. 87, p. 1075–1099, doi:10.2110/jsr.2017.59.

Durkin, P.R., Hubbard, S.M., Holbrook, J., Boyd, R., 2018, Evolution of fluvial meander-belt deposits and implications for the completeness of the stratigraphic record, Geological Society of America Bulletin.

Edmonds, D.A., Hajek, E.A., Downton, N., Bryk, A.B., 2016, Avulsion flow-path selection on rivers in foreland basins. Geology, 44(9), pp.695-698.

Edmonds, D.A., Valenza, J., Roy, S., Hwang, T., 2018, Fingerprinting River Avulsions, in AGU Fall Meeting Abstracts.

Fontana, A., Mozzi, P., Bondesan, A., 2008, Alluvial megafans in the Venetian–Friulian Plain (north-eastern Italy): evidence of sedimentary and erosive phases during Late Pleistocene and Holocene, Quaternary International, 189(1), pp.71-90.

Friend, P.F., Slater, M.J., Williams, R.C., 1979, Vertical and lateral building of river sandstone bodies, Ebro Basin, Spain. Journal of the Geological Society, 136(1), pp.39-46.

Geologic Map of New Mexico, New Mexico Bureau of Geology and Mineral Resources, 2003, Scale 1:500,000.

Gibling, M.R., Tandon, S.K., Sinha, R., and Jain, M., 2005, Discontinuity-Bounded Alluvial Sequences of the Southern Gangetic Plains, India: Aggradation and Degradation in Response to Monsoonal Strength: Journal of Sedimentary Research, v. 75, p. 369–385, doi:10.2110/jsr.2005.029.

Gibling, M.R., 2006, Width and thickness of fluvial channel bodies and valley fills in the geological record: a literature compilation and classification, Journal of sedimentary Research, 76(5), pp.731-770.

Gibling, M.R., Fielding, C.R., Sinha, R., Davidson, S.K., Leleu, S., North, C.P., 2011, Alluvial valleys and alluvial sequences: towards a geomorphic assessment, From River to Rock Record: The Preservation of Fluvial Sediments and Their Subsequent Interpretation: SEPM, Special Publication, 97, pp.423-447.

Green, G.N., 1992, The digital geologic map of Colorado in ARC/INFO format.

Hartley, A. J., Owen, A., Swan, A., Weissmann, G. S., Holzweber, B. I., Howell, J., Scuderi, L., 2015, Recognition and importance of amalgamated sandy meander belts in the continental rock record, Geology, 43(8), 679-682.

Hobbs, K. M., 2016, Sedimentation, pedogenesis, and paleoclimate conditions in the Paleocene San Juan basin, New Mexico, U.S.A (Order No. 10155515). Available from Dissertations & Theses @ University of New Mexico; ProQuest Dissertations & Theses Global. (1836821405). Retrieved from http://libproxy.unm.edu/login?url=https://search-proquest-com.libproxy.unm.edu/docview/1836821405?accountid=14613

Hofmann, M.H., Wroblewski, A., and Boyd, R., 2011, Mechanisms Controlling the Clustering of Fluvial Channels and the Compensational Stacking of Cluster Belts: Journal of Sedimentary Research, v. 81, p. 670–685, doi:10.2110/jsr.2011.54.

Holbrook, J., 2001, Origin, genetic interrelationships, and stratigraphy over the continuum of fluvial channel-form bounding surfaces: an illustration from middle Cretaceous strata, southeastern Colorado, Sedimentary Geology, 144(3-4), 179-222.

Huerta, P., Armenteros, I., Silva, P.G., 2011, Large-scale architecture in non-marine basins: the response to the interplay between accommodation space and sediment supply, Sedimentology, 58(7), pp.1716-1736.

Jones, H.L., and Hajek, E.A., 2007, Characterizing avulsion stratigraphy in ancient alluvial deposits: Sedimentary Geology, v. 202, p. 124–137, doi:10.1016/j.sedgeo.2007.02.003.

Kjemperud, A. V., Schomacker, E. R., Cross, T. A., 2008, Architecture and stratigraphy of alluvial deposits, Morrison formation (Upper Jurassic), Utah. AAPG bulletin, 92(8), 1055-1076.

Leeder, M.R., 2009, Sedimentology and Sedimentary Basins: from Turbulence to Tectonics, 1ed, Willey-Blackwell, 768pp.

Leslie, C., Peppe, D., Williamson, T., Bilardello, D., Heizler, M., Secord, R., Leggett, T., 2018, High-resolution magnetostratigraphy of the Upper Nacimiento Formation, San Juan Basin, New Mexico, USA: Implications for basin evolution and mammalian turnover, American Journal of Science, 318(3), pp.300-334.

Mackey, S. D., Bridge, J. S., 1995, Three-dimensional model of alluvial stratigraphy: theory and application. Journal of Sedimentary Research B65:7–31.

Miall, A.D., 1996. The Geology of Fluvial Deposits: Sedimentary Facies, Basin Analysis and Petroleum Geology. Springer, Berlin, pp. 592.

Moraes, Marco A.S., de Ros, L.F. Special Publication - Society of Economic Paleontologists and Mineralogists: Depositional, infiltrated and authigenic clays in fluvial sandstones of the Jurassic Sergi Formation, Reconcavo Basin, northeastern Brazil:

Nichols, G., 2013, Sedimentology and Stratigraphy: Somerset, Wiley.

Nichols, G., 2015, Stratigraphic Architecture of Fluvial Distributive Systems in Basins of Internal Drainage. In AAPG Annual Convention and Exhibition, Denver, Colorado.

Owen, A., Nichols, G.J., Hartley, A.J., Weissmann, G.S., 2017, Vertical trends within the prograding Salt Wash distributive fluvial system, SW United States, Basin Research, 29(1), pp.64-80.

Paolo C., Claudio M., Claudio R., Roberto S., Marco T., 1999, Preserving attribute values on simplified meshes by resampling detail textures, The Visual Computer, 15 (9).

Pickel, A., Frechette, J.D., Comunian, A., Weissmann, G.S., 2015, Building a training image with Digital Outcrop Models, Journal of Hydrology, 531, pp.53-61.

Ridgley, J.L., Condon, S.M., Dubiel, R.F., Charpentier, R.R., Cook, T.A., Crovelli, R.A., Klett, T.R., Pollastro, R.M. and Schenk, C.J., 2002, Assessment of undiscovered oil and gas resources of the San Juan Basin Province of New Mexico and Colorado (No. 147-02).

Sikkink, P.G., 1987, Lithofacies relationships and depositional environment of the Tertiary Ojo Alamo Sandstone and related strata, San Juan basin, New Mexico and Colorado, Geological Society of America Special Papers, 209, pp.81-104.

Slingerland, R., Smith, N.D., 2004, River avulsions and their deposits, Annu. Rev. Earth Planet. Sci., 32, pp.257-285.

Taylor, L.H., 1977, Geochronology of Torrejonian sediments, Nacimiento Formation, San Juan Basin, New Mexico (Doctoral dissertation, University of Arizona).

Valenza, J.M., Edmonds, D.A., Roy, S., and Hwang, T.H., 2018, Fingerprinting river avulsions, doi:10.1130/abs/2018am-322382.

Ventra, D., and Nichols, G.J., 2014, Autogenic dynamics of alluvial fans in endorheic basins: Outcrop examples and stratigraphic significance: Sedimentology, v. 61, p. 767–791, doi:10.1111/sed.12077.

Weissmann, G.S., Mount, J.F., Fogg, G.E., 2002, Glacially driven cycles in accumulation space and sequence stratigraphy of a stream-dominated alluvial fan, San Joaquin Valley, California, USA, Journal of Sedimentary Research, 72(2), pp.240-251.

Weissmann, G.S., Zhang, Y., Fogg, G.E.,Mount, J.F., 2004. Influence of incised-valley-fill deposits on hydrogeology of a stream-dominated alluvial fan. In: Bridge, J.S., Hyndman, D.W. (Eds.), Aquifer Characterization, SEPM (Society for Sedimentary Geology), Special Publication 80, pp. 15–28.

Weissmann, G.S., Hartley, A.J., Nichols, G.J., Scuderi, L.A., Olson, M., Buehler, H., Banteah, R., 2010, Fluvial form in modern continental sedimentary basins: distributive fluvial systems, Geology, 38(1), pp.39-42.

Weissmann, G.S., Hartley, A.J., Scuderi, L.A., Nichols, G.J., Davidson, S.K., Owen, A., Atchley, S.C., Bhattacharyya, P., Chakraborty, T., Ghosh, P., Nordt, L.C., 2013, Prograding distributive fluvial systems: geomorphic models and ancient examples, In New Frontiers in Paleopedology and Terrestrial Paleoclimatology (Vol. 104, pp. 131-147), SEPM, Special Publication 104.

Weissmann, G.S., Hartley, A.J., Scuderi, L.A., Nichols, G.J., Owen, A., Wright, S., Felicia, A.L., Holland, F., Anaya, F.M.L., 2015, Fluvial geomorphic elements in modern sedimentary basins and their potential preservation in the rock record: a review, Geomorphology, 250, pp.187-219.

Williamson, T. E., 1993, The beginning of the age of mammals in the San Juan basin: Biostratigraphy and evolution of Paleocene mammals of the Nacimiento Formation (Order No. 9421268). Available from Dissertations & Theses @ University of New Mexico; ProQuest Dissertations & Theses Global. (304040817). Retrieved from http://libproxy.unm.edu/login?url=https://search-proquest-com.libproxy.unm.edu/docview/304040817?accountid=14613

Williamson, T.E., 1996, The beginning of the age of mammals in the San Juan Basin, New Mexico: Biostratigraphy and evolution of Paleocene mammals of the Nacimiento Formation: New Mexico Museum of Natural History and Science, Bulletin 8, 141 p.

Williamson, T.E., and Lucas, S.G., 1992, Stratigraphy and mammalian biostratigraphy of the Paleocene Nacimiento Formation, southern San Juan Basin, New Mexico: New Mexico Geological Society Guidebook, v. 43, p. 265-296.

Willis, B., 1993, Ancient river systems in the Himalayan foredeep, Chinji Village area, northern Pakistan, Sedimentary Geology, 88(1-2), pp.1-76.